# CHARACTERIZATION OF POWER QUALITY DISTURBANCES USING SIGNAL PROCESSING AND SOFT COMPUTING TECHNIQUES

*A thesis submitted to NIT Rourkela*

*in partial fulfilment of the requirement for the award of the Degree of*

Master of Technology

*In*

Power Control & Drives

*By*

**DEBASIS CHOUDHURY**

**Roll No-210EE2101**


**Department of Electrical Engineering**

**National Institute of Technology**

**Rourkela-769008 May, 2013**

# CHARACTERIZATION OF POWER QUALITY DISTURBANCES USING SIGNAL PROCESSING AND SOFT COMPUTING TECHNIQUES

*A thesis submitted to NIT Rourkela*

*in partial fulfilment of the requirement for the award of the Degree of*

Master of Technology

*In*

Power Control & Drives

*By*

**DEBASIS CHOUDHURY**

Under the Guidance of

**Prof. Sanjeeb Mohanty**

**Department of Electrical Engineering**

**National Institute of Technology**

**Rourkela-769008 May, 2013**


# National Institute of Technology Rourkela

## CERTIFICATE

This is to certify that the thesis entitled, **"Characterization of Power Quality Disturbances using Signal Processing and Soft Computing Techniques"** submitted by **Debasis Choudhury (Roll No. 210EE2101)** in partial fulfillment of the requirements for the award of Master of Technology Degree in Electrical Engineering with specialization in Power Control & Drives during 2012 -2013 at the National Institute of Technology, Rourkela is an authentic work carried out by him under my supervision and guidance.

To the best of my knowledge, the matter embodied in the thesis has not been submitted to any other University / Institute for the award of any Degree or Diploma.

Date

Prof. Sanjeeb Mohanty
Department of Electrical Engineering
National Institute of Technology
Rourkela-769008

# ACKNOWLEDGEMENTS

I would like to express my sincere gratitude to my supervisor **Prof. Sanjeeb Mohanty** for his guidance, encouragement, and support throughout the course of this work. It was an invaluable learning experience for me to be one of his students. As my supervisor his insight, observations and suggestions helped me to establish the overall direction of the research and contributed immensely for the success of this work.

I express my gratitude to **Prof. A. K. Panda,** Head of the Department, Electrical Engineering for his invaluable suggestions and constant encouragement all through this work.

My thanks are extended to my colleagues in power control and drives, who built an academic and friendly research environment that made my study at NIT, Rourkela most fruitful and enjoyable.

I would also like to acknowledge the entire teaching and non-teaching staff of Electrical department for establishing a working environment and for constructive discussions.

Finally, I am always indebted to all my family members, especially my parents, for their endless support and love.

**Debasis Choudhury**
**Roll - no.:- 210EE2101**

# Contents

# Abstract

The power quality of the electric power has become an important issue for the electric utilities and their customers. In order to improve the quality of power, electric utilities continuously monitor power delivered at customer sites. Thus automatic classification of distribution line disturbances is highly desirable. The detection and classification of the power quality (PQ) disturbances in power systems are important tasks in monitoring and protection of power system network. Most of the disturbances are non-stationary and transitory in nature hence it requires advanced tools and techniques for the analysis of PQ disturbances. In this work a hybrid technique is used for characterizing PQ disturbances using wavelet transform and fuzzy logic. A no of PQ events are generated and decomposed using wavelet decomposition algorithm of wavelet transform for accurate detection of disturbances. It is also observed that when the PQ disturbances are contaminated with noise the detection becomes difficult and the feature vectors to be extracted will contain a high percentage of noise which may degrade the classification accuracy. Hence a Wavelet based de-noising technique is proposed in this work before feature extraction process. Two very distinct features common to all PQ disturbances like Energy and Total Harmonic Distortion (THD) are extracted using discrete wavelet transform and is fed as inputs to the fuzzy expert system for accurate detection and classification of various PQ disturbances. The fuzzy expert system not only classifies the PQ disturbances but also indicates whether the disturbance is pure or contains harmonics. A neural network based Power Quality Disturbance (PQD) detection system is also modeled implementing Multilayer Feedforward Neural Network (MFNN).

# List of Figures

# List of Tables

# List of Abbreviations

| | |
|---|---|
| ANN | Artificial Neural Network |
| BPA | Back Propagation Algorithm |
| CWT | Continuous Wavelet Transform |
| DWT | Discrete Wavelet Transform |
| FL | Fuzzy Logic |
| FT | Fourier Transform |
| MAE | Mean Absolute Error |
| MFNN | Multilayer Feedforward Neural Network |
| NN | Neural Network |
| MSE | Mean Square Error |
| PE | Processing Elements |
| PQ | Power Quality |
| PQD | Power Quality Disturbance |
| RMS | Root Mean Square |
| SNR | Signal to Noise Ratio |
| STFT | Short Time Fourier Transform |
| THD | Total Harmonic Distortion |
| WT | Wavelet Transform |

## 1.1 Introduction

Now-a-days the equipment used with electrical utility are far more sensitive to power quality (PQ) variation than in the past. The equipments used are mostly digital or microprocessor based containing power electronic components which are sensitive to power disturbances. The Poor power quality can cause some serious problems to the equipment such as short lifetime, malfunctioning, instabilities, interruption and reduced efficiency etc. Hence both electrical utilities suppliers and customers are becoming aware of the effects of power quality of power supply on load equipment. As a result power quality research is gaining interest and from the extensive research it is found that the main causes behind the poor power quality are power line disturbances such as Voltage Sag, Voltage Swell, Interruption, Oscillation and Harmonics etc. Therefore mitigation of PQ disturbances becomes prime concern in improving the power quality but before that it is essential to monitor and detect the type of disturbance that has occurred in power line so that the sources of disturbance can be identified and appropriate measures can be taken to mitigate the problem. Most of the disturbances are non-stationary in nature hence it requires advanced tools and techniques for the analysis of PQ disturbances. A normal Fourier transform is not a suitable tool for analysis of PQ disturbances as it provides only spectral information of the signal without the time localization information which is required to find the start time and end time as well as the interval of the disturbance [1].The Short Time Fourier Transform (STFT) is another signal processing technique but it is well suited for stationary signals where the frequency does not vary with time [2-4]. However for non-stationary signals STFT does not recognize the signal dynamics due to the limitation of fixed window width [2]. The time frequency analysis technique is more appropriate for analysing non-stationary signal because it provides both time and spectral information of the signal. The Discrete Wavelet Transform (DWT) is preferred because it employs a flexible window to detect the time frequency variations which results in a better time-frequency resolution [5].

## 1.2 Literature Survey

Extensive research works have been pursued in the area of application of digital signal processing techniques to power quality event analysis.Santoso et al.[6] used the Wavelet Transform (WT) in combination with Fourier transform to extract unique features from the voltage and current waveforms that characterize power quality events. The Fourier transform is used to characterize steady state phenomena and the WT is applied to transient phenomena.

Wright et al. [2] have applied Short time Fourier transform (STFT) which is another signal processing technique but it is well suited for stationary signals where the frequency does not vary with time. However for non-stationary signal STFT does not recognize the signal dynamics due to the limitation of fixed window width. The WT is an excellent tool for analysing non stationary signals and it overcomes the drawback of STFT. It decomposes the signal into time scale representation rather than time frequency representation. The DWT is a powerful computing and mathematical tool which has been used independently in applied mathematics, signal processing and others. In wavelet analysis, the use of a fully scalable modulated window can solve the signal cutting problem. The main idea of this method is to look at the signal at different scales or resolution. Hence the WT has been explored extensively in various studies as an alternative to STFT [7-9].Abdelazeem et al [7] presented a hybrid technique for detecting and characterizing power quality disturbances using WT, kalman filter and fuzzy logic.L.C Saikia et al [8] have proposed a technique based on the WT and the artificial neural network for characterizing power quality disturbances. The Support Vector Machine (SVM) was introduced in several literatures [10], [11] as a tool for the classification. However there were still some incorrect classification cases because of the sub band overlapping of different power quality disturbances. In the recent past wavelet transform in conjunctions with artificial intelligence technique is used popularly for characterizing power quality. Some literatures are reported in [12-18] but there exists a difficulty in characterizing i.e. the sampling signals often have noisy component, the locations of start-time and end-time are hard to get. The Wavelet is an effective tool for those non-stationary signal processing and has been used in this field. Wei Bing Hu et al [20] have developed a technique based on the wavelet transform for de-noising of power quality event as the presence of noise in power quality events may degrade the classification accuracy. To overcome the difficulties of extraction of the feature vector of the disturbance out of the noises in a low SNR environment, a de-noising technique is proposed. Gu jie [22] has also proposed a wavelet threshold based de-noising technique for power quality disturbances.Chuah Heng Keow et al [21] have proposed a scheme for enhancing power quality problem classification based on the wavelet transform and a rule-based method.

## 1.3 Motivation and Objective of the Work

From the literature survey it is clearly understood that the discrete wavelet transformation (DWT) is a powerful computing and mathematical tool which have been used independently in applied mathematics, signal processing and more importantly in the area of power quality

analysis. The main cause behind the degradation of power quality is the power line disturbances in order to find a corrective measure for the above problem one needs to detect and classify the power quality disturbances accurately for further processing and research. This provides sufficient motivation to work on the above area using the advanced signal processing technique and artificial intelligence. The main idea of this work is to look at the signal at different scales or resolution. In this work, the generated signals are decomposed into different levels through wavelet transform and any change in smoothness of the signal is detected. The Different level gives different resolution. This work shows that each power quality disturbance has unique deviation from the pure sinusoidal waveform and this is adopted to provide a reliable classification of different type of disturbance. The objective of this work is

- To generate different power quality disturbances
- To detect the disturbances using wavelet transform
- To de-noise the disturbances polluted with noise
- To model a PQ disturbances detection system using artificial neural network
- Classification of PQ disturbances using fuzzy expert system

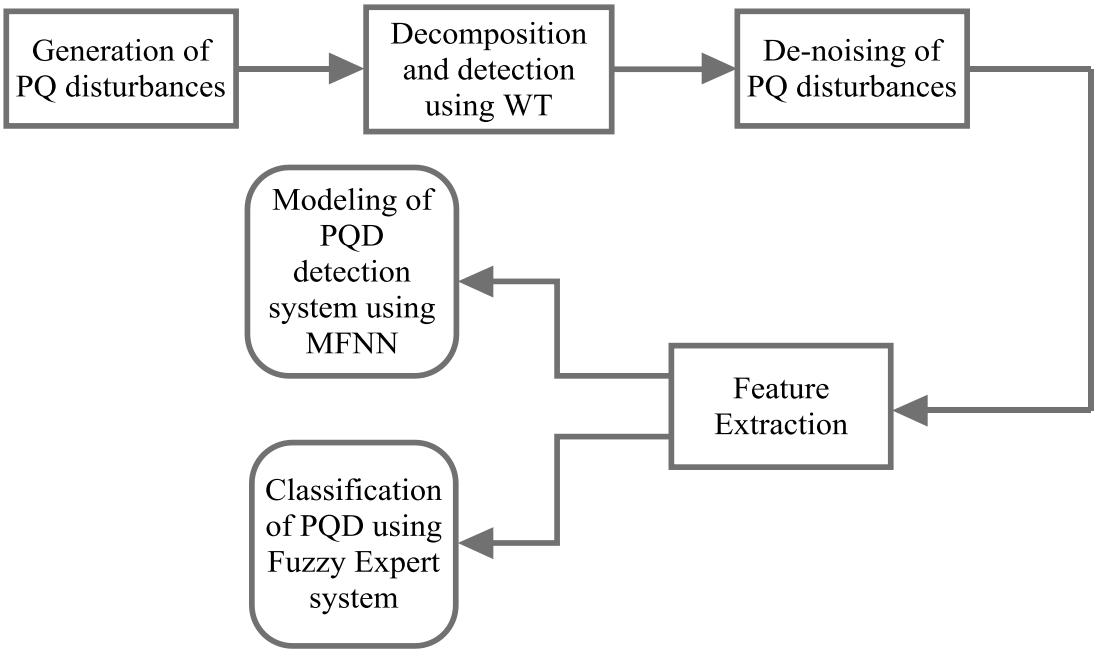


**Figure1.1 Basic block diagram of the method adopted**

Figure 1.1 shows the basic block diagram of the method adopted in this work. In the first stage the different power quality disturbances are generated and in the second stage they are

decomposed through the wavelet transform and the instant of the disturbance and the type of disturbance is detected. In the third stage the PQ disturbances are de-noised if noise is present because PQ disturbances combined with noises may degrade the classification accuracy as the feature vector will be contaminated with high percentage of noise. In the fourth stage the features like energy and total harmonic distortion (THD) are extracted from the detected noise free signal. In the fifth and final stage the above mentioned features are used to classify different PQ disturbances using fuzzy expert system and a PQD detection system is modeled using multilayer Feedforward neural network.

## 1.4 Thesis Layout

**Chapter 1** reviews the literature on various power quality issues and characterization of power quality disturbances. The Literatures are also reviewed on the wavelet transform as a tool for analysing different power quality events in conjunction with the artificial intelligence technique. The Motivation and objective along with brief description of the work is presented.

**Chapter 2** describes the mechanism of wavelet transform and decomposition algorithm in detail and then different PQ disturbances are simulated and decomposed using wavelet decomposition algorithm and successful detection is carried out. Various decomposition parameters like choice of mother wavelet and selection of maximum decomposition levels are mentioned. Also the problems regarding detection in presence of noise are discussed.

**Chapter 3** employs wavelet based de-noising technique for extraction of noise free PQ disturbances. The Various issues regarding de-noising like selection of thresholding function, thresholding rules are discussed and various performance indices for characterizing an effective de-noising technique are discussed and evaluated.

**Chapter 4** deals with the feature extraction. The THD and Energy are used as the feature vector for preparing the database of different PQ disturbances to be used for training of the neural network for modeling a power quality disturbance (PQD) detection system and input to the fuzzy expert system.

**Chapter 5** employs a Multilayer Feedforward Neural Network (MFNN) for modeling a PQD detection system. Features extracted in chapter 4 are used as input-output data for training purposes and mean square error and mean absolute error were obtained.

**Chapter 6** employs a fuzzy expert system for classifying different PQ disturbances and classification accuracy of each PQ disturbance was found out.

**Chapter 7** summarizes the results obtained in each chapter and future scope of work is discussed in brief.

## 2.1Introduction

Now-a-days with the advent of the digital techniques, the PQ disturbances are monitored onsite and online. Recently the wavelet transform (WT) has emerged as a powerful tool for the detection of PQ disturbances. The Wavelet transform uses wavelet function as the basis function which scales itself according to the frequency under analysis. The scheme shows better results because the basis function used in the WT is a wavelet instead of an exponential function used in FT and STFT. Using the WT the signal is decomposed into different frequency levels and presented as wavelet coefficients. Depending on the types of signal, continuous wavelet transform (CWT) and discrete wavelet transform (DWT) are employed. For continuous time signal, CWT based decomposition is adopted and for discrete time signal DWT based decomposition is employed. However in this work all the signals shown are discrete in nature hence DWT based decomposition is employed here.In this part of the work different PQ disturbances such as Sag, Swell, Interruption, Sag with harmonics and Swell with harmonics are generated using MATLAB and then decomposed using decomposition algorithm of WT and point of actual disturbance is located and type of disturbance is detected.

## 2.2 Discrete Wavelet Transform (DWT)

Basically the DWT evaluation has two stages. The first stage is the determination of wavelet coefficients $h_d(n)$ and $g_d(n)$.These coefficients represent the given signal *X(n)* in the wavelet domain. From these coefficients second stage is achieved with the calculation of both the approximated and detailed version of the original signal, these wavelet coefficients are called $cA_1$ (n) and $cD_1$ (n) as defined below.

$$cA_1(n) = \sum_k S(n).h_d(-k+2n) \tag{2.1}$$

$$cD_1(n) = \sum_k S(n).g_d(-k+2n) \tag{2.2}$$

The same process is adopted to calculate $cA_2$ (n) and $cD_2$ (n) associated with level 2 decomposition of the signal and the process goes on. The above algorithm is shown in Figure 2.1.First of all the original signal *X(n)* is passed through a band pass filter which is the combination of a set of low pass and high pass filter followed by a sub-sampling of two in each stage in accordance with Nyquist's rule to avoid data redundancy problem. Once all the

wavelet coefficients are known the DWT in time domain can be determined by reconstructing the corresponding wavelet coefficients at different levels. The reconstruction algorithm is shown in Figure 2.3 which is just the reverse process of Wavelet decomposition. The wavelet transform (WT) of a signal *X(t*) is stated as

$$WT_x(a, b) = \int_{-\infty}^{\infty} X(t)\Psi_{a,b}^{*}dt \quad (2.3)$$

Where $\Psi_{a,b}(t) = \Psi((t-b)/a)/\sqrt{a}$ (2.4)

is a scaled and shifted version of the mother wavelet Ψ(t).The parameter *a* corresponds to scale and frequency domain property of Ψ(t).The parameter *b* corresponds to time domain property of Ψ(t) .In addition $1/\sqrt{a}$ is the normalization value of $\Psi_{a,b}(t)$ for having spectrum power as same as mother wavelet in every scale. The DWT is introduced by considering sub band decomposition using the digital filter equivalent to DWT.The filter bank structure is shown in Figure 2.1.The Band pass filter is implemented as a low pass and high pass filter pair which has mirrored charecteristics.While the low pass filter approximates the signal. The high pass filter provides the details lost in the approximation. The approximations are low frequency high scale component whereas the details are high frequency low scale component.

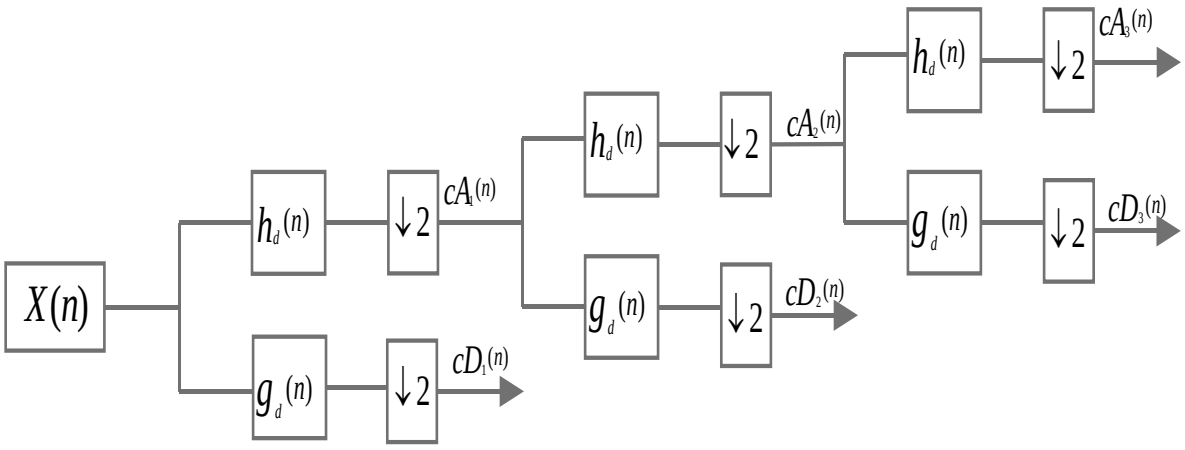


**Figure 2.1 Decomposition algorithm**

Where

$h_d[n]$ = Impulse response of Low pass filter

$g_d[n]$ = Impulse response of High pass filter

X(n) = Discretized original signal

$cA_1(n)$ =Approximate coefficient of level 1 decomposition/output of first LPF

$cD_1(n)$ = Detail coefficient of level 1 decomposition/output of first HPF

$cA_2(n)$ =Approximate coefficient of level 2 decomposition/output of $2^{nd}$ LPF

$cD_2(n)$ = Detail coefficient of level 2 decomposition/output of $2^{nd}$ HPF

$cA_3(n)$ =Approximate coefficient of level 3 decomposition/output of $3^{rd}$ LPF

$cD_3(n)$ = Detail coefficient of level 3 decomposition/output of $3^{rd}$ HPF

Figure 2.2 shows the more simplified diagram of decomposition algorithm of the signal *X(n)* which is decomposed up to level 3 for demonstrating how the original signal *X(n)* is related to the decomposed version of the same in terms of approximate and detail coefficients at each level.

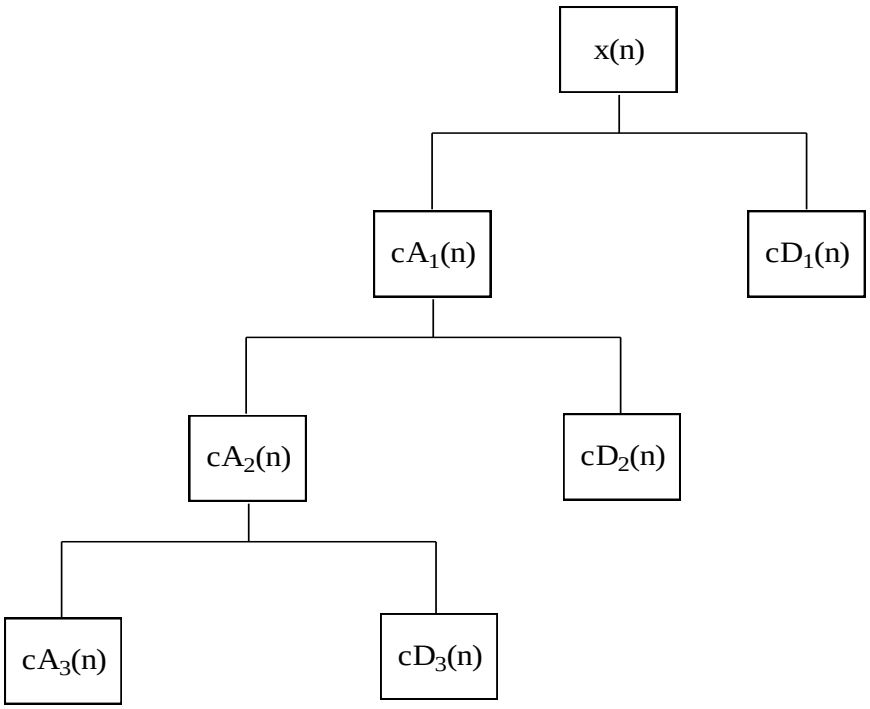


**Figure 2.2 Decomposition of a signal X(n) up to level 3**

**Level 1 decomposition**

$X(n) = cA_1(n) + cD_1(n)$

**Level 2 decomposition**

$X(n) = cA_2(n) + cD_2(n) + cD_1(n)$

**Level 3 decomposition**

$X(n) = cA_3(n) + cD_3(n) + cD_2(n) + cD_1(n)$

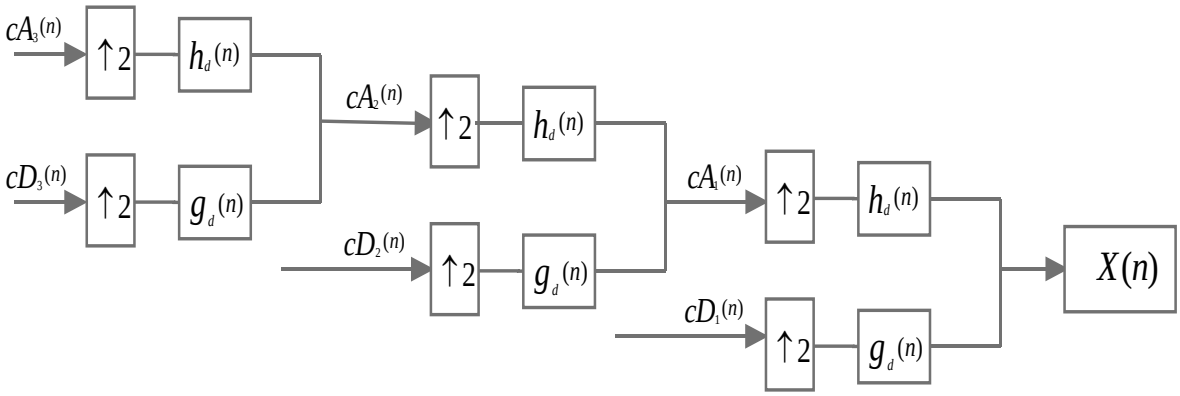


**Figure 2.3 Reconstruction algorithm**

### 2.2.1 Choice of Mother Wavelet

The selection of mother wavelet is an important issue for decomposition of PQ disturbances as the proper selection of mother wavelet results in accurate detection of disturbances. The original signal to be decomposed is multiplied with the selected mother wavelet to obtain the scaled and translated version of the original signal at different levels. There are several mother wavelets such as Daubechies, Morlet, Haar, Symlet etc. exists in wavelet library but literatures revealed that for power quality analysis Daubechies wavelet gives the desired result. Again the Daubechies wavelet has several orders such as Db2, Db3, Db4, Db5 Db6, Db7 Db8, and Db10etc.The Daubechies wavelets with 4, 6, 8, and10 filter coefficients work well in most disturbance cases. Based on the detection problem, the power quality disturbances can be classified into two types, fast and slow transients. In the fast transient case the waveforms are marked with sharp edges, abrupt and rapid changes, and a fairly short duration in time. In this case Daub4 and Daub6 gives good result due to their compactness. In slow transient case Daub8 and Daub10 shows better performance as the time interval in integral evaluated at point n is long enough to sense the slow changes.

### 2.2.2 Selection of maximum decomposition level

In the DWT, the maximum decomposition level of a signal is determined by $J_{max} = fix\ (log_2\ n)$ where $n$ is the length of the signal; *fix* rounds the value in the bracket to its nearest integer. However in this work as the MATLAB wavelet toolbox is employed, the signal

length at the highest level of decomposition should not be less than the length of the wavelet filter being used. So the maximum decomposition level $J_{max}$ for a signal is given as

$$J_{max} = fix\left(log_2\left(\frac{N}{N_w} - 1\right)\right) \quad (2.5)$$

Where *N*= Length of the signal, *Nw*= Length of the decomposition filter associated with the chosen mother wavelet. However in practice maximum decomposition level for a wavelet based de-noising is selected according to the convenience and requirement.

## 2.3 Generation of PQ disturbances

The various power quality disturbances such as Sag, Swell, Interruption, and Sag with harmonics and Swell with harmonics are generated with different magnitudes using MATLAB.

### 2.3.1 Signal specification

$T_s$ (time period) =0.5 sec, $f_s$ (sampling frequency) =6.4 KHz, f=50Hz, No of cycles=25, No of samples/cycle=128, Total Sampling points=3200.Duration of disturbance=0.2 second. The interval of disturbance from 0.2 to 0.4 second of time which is between 1250 to 2500 sampling points.

### 2.3.2 Parametric model of PQ disturbances

**Table 2.1 Equations and parameter variations for PQ signals**

| PQ disturbance | Model | Parameter variations |
|---|---|---|
| Voltage Sag | $X(t) = A\left(1 - \alpha\left(u(t-t_1) - u(t-t_2)\right)\right)\sin(\omega t)$<br>$t_1 < t_2, u(t) = 1\ if\ t \geq 0,$<br>$u(t) = 0\ if\ t < 0$ | $0.1 \leq \alpha \leq 0.9$<br>$T \leq t_2\text{-}t_1 \leq 10T$ |
| Voltage Swell | $X(t) = A\left(1 + \alpha\left(u(t-t_1) - u(t-t_2)\right)\right)\sin(\omega t)$<br>$t_1 < t_2, u(t) = 1\ if\ t \geq 0,$<br>$u(t) = 0\ if\ t < 0$ | $0.1 \leq \alpha \leq 0.9$<br>$T \leq t_2\text{-}t_1 \leq 10T$ |
| Interruption | $X(t) = A\left(1 - \alpha\left(u(t-t_1) - u(t-t_2)\right)\right)\sin(\omega t)$ | $0.01 \leq \alpha \leq 0.09$<br>$T \leq t_2\text{-}t_1 \leq 10T$ |

| | | |
|---|---|---|
| Voltage sag with harmonics | $X(t) = A\left(1 - \alpha\left(u(t-t_1) - u(t-t_2)\right)\right)(\alpha_1 \sin(\omega t) + \alpha_2 \sin(2\omega t) + \alpha_3 \sin(3\omega t) + \alpha_5 \sin(5\omega t) + \alpha_7 \sin(7\omega t))$ | $\alpha_1$=1.0<br>$0.0 \leq \alpha_2, \alpha_3, \alpha_5$ and $\alpha_7 \leq 0.3$<br>$0.1 \leq \alpha \leq 0.9$<br>$T \leq t_2$-$t_1 \leq 10T$ |
| Voltage swell with harmonics | $X(t) = A\left(1 + \alpha\left(u(t-t_1) - u(t-t_2)\right)\right)(\alpha_1 \sin(\omega t) + \alpha_2 \sin(2\omega t) + \alpha_3 \sin(3\omega t) + \alpha_5 \sin(5\omega t) + \alpha_7 \sin(7\omega t))$ | $\alpha_1$=1.0<br>$0.0 \leq \alpha_2, \alpha_3, \alpha_5$ and $\alpha_7 \leq 0.3$<br>$0.1 \leq \alpha \leq 0.9$<br>$T \leq t_2$-$t_1 \leq 10T$ |
| Voltage distortion | $X(t) = A\,(\alpha_1 \sin(\omega t) + \alpha_2 \sin(2\omega t) + \alpha_3 \sin(3\omega t) + \alpha_5 \sin(5\omega t) + \alpha_7 \sin(7\omega t))$ | $\alpha_1$=1.0<br>$\alpha_2$-$\alpha_7$=(0.0-0.3) |

The parameter α represents the level of sag or swell in the first two types of disturbances. The unit step function *u(t)* in the whole table provides the duration of disturbances present in the pure sine waveform. During the generation of the disturbance signal from the parametric model, the value of α and the position of *u(t)* has been varied suitably, so that a large number of signals can be obtained with varying magnitude (by changing α*)* on different points on the wave (by changing the parameters $t_1$ and $t_2$) and the duration of the disturbance ($t_2$-$t_1$). The point on the wave *is* the instant on the sinusoid when a disturbance begins and is controlled by the position of the unit step function *u(t).* As the real PQ disturbance signals may have any point on the wave which is beyond control, hence we have generated a variety of disturbances having different points on the wave duration of disturbance and magnitudes. The harmonic signal consists of a combination of second-, third-, fifth- and seventh-order harmonics. The momentary interruption with parameter α is taken for varying the amplitude during interruption. Using the above parametric model hundred no of PQ events in each class of the disturbance are generated.

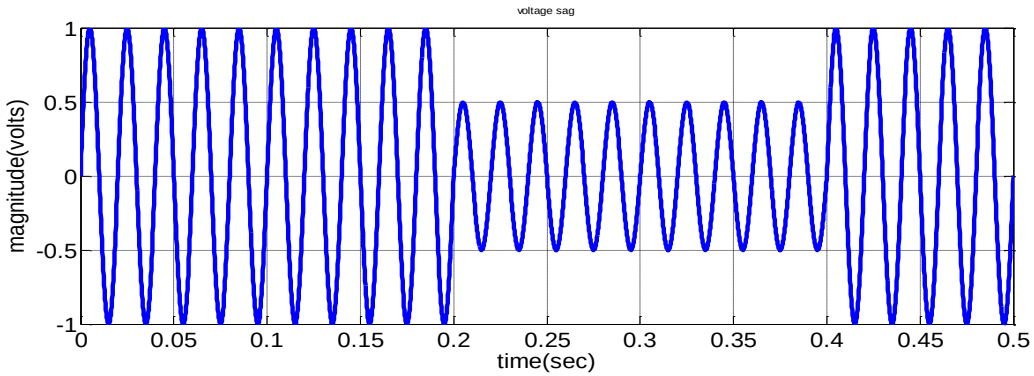


**Figure 2.4 (a) Voltage sag**

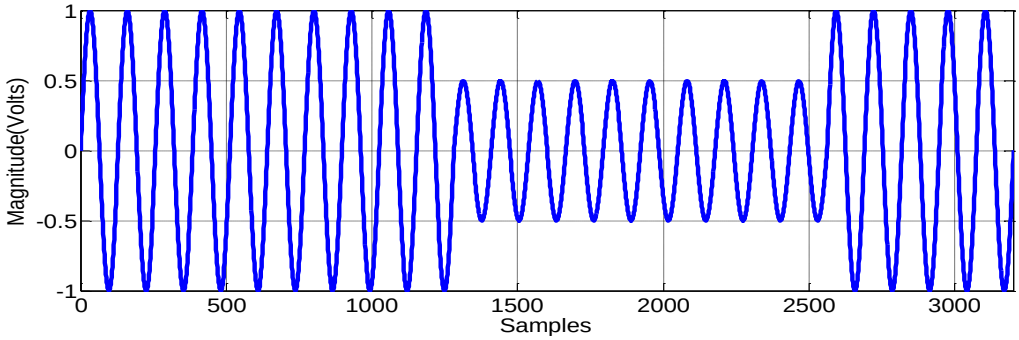


**Figure 2.4 (b) Voltage sag**

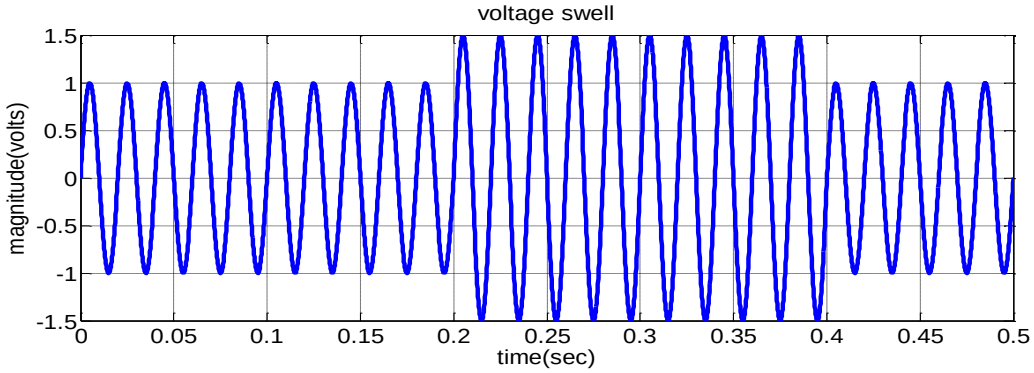


**Figure 2.5 (a)**

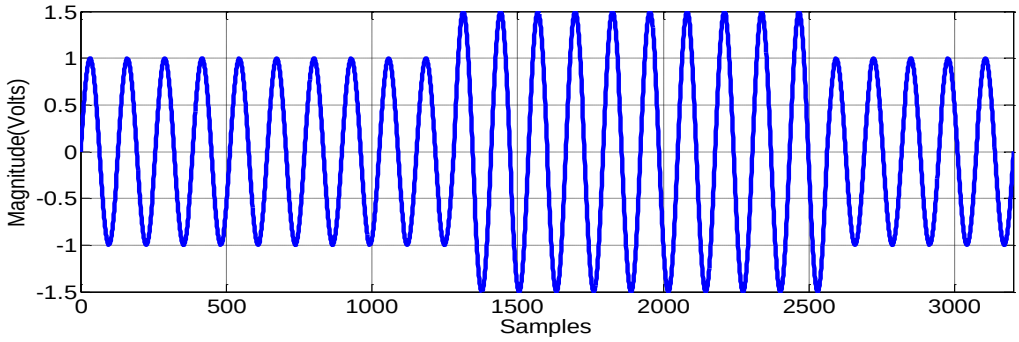


**Figure 2.5 (b)**

**Figure 2.5 (a) and (b) Swell disturbance with $f_s$=6.4 KHz**

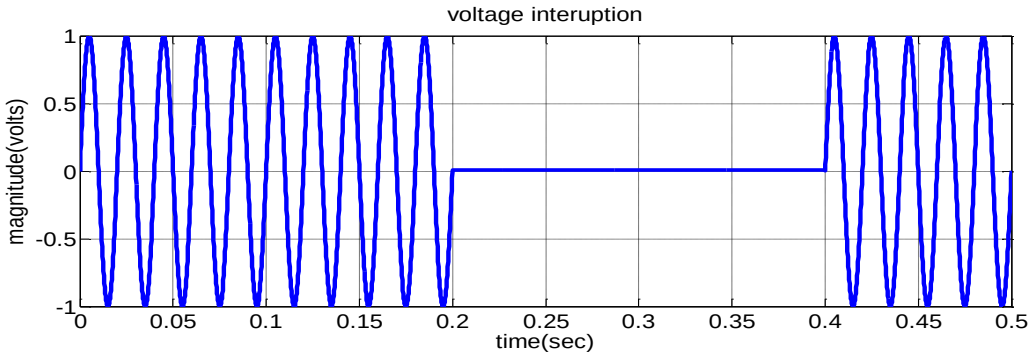


**Figure 2.6 (a)**

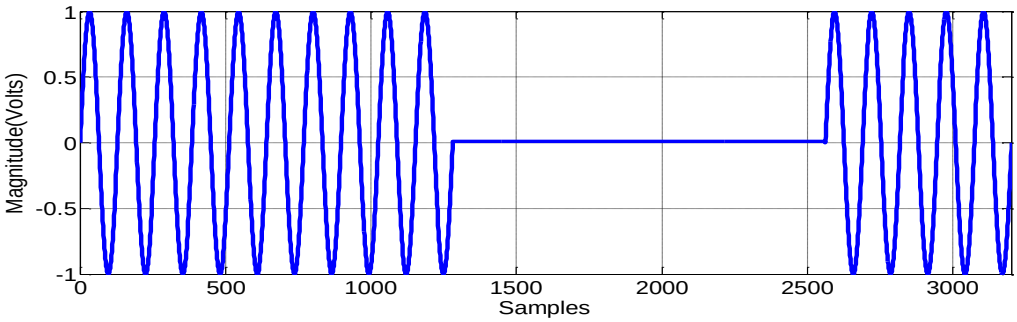


**Figure 2.6 (b)**

**Figure 2.6 (e) and (f) Voltage Interruption with $f_s$=6.4 KHz**

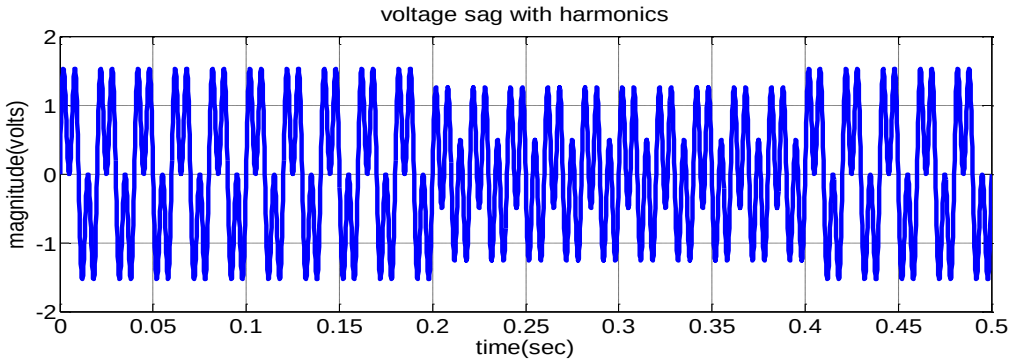


**Figure 2.7 (a)**

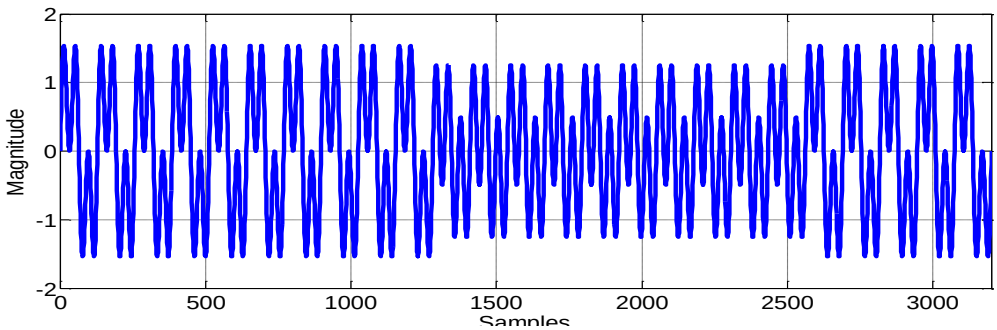


**Figure 2.7 (b)**

**Figure 2.7 (a) and (b) Voltage Sag with 3rd Harmonic**

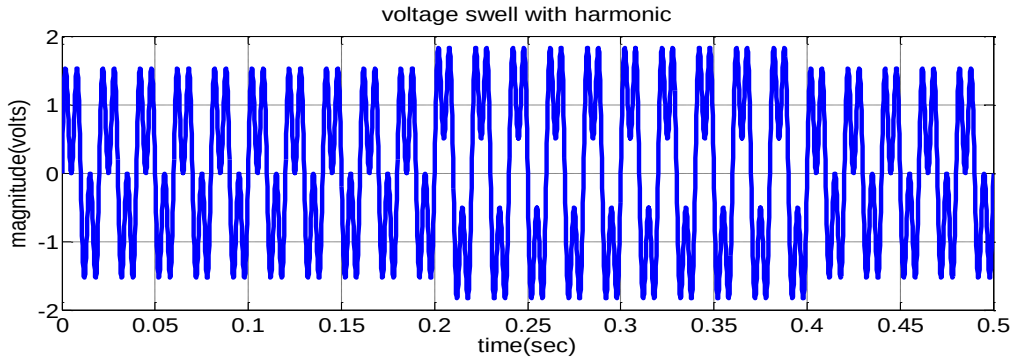


**Figure 2.8 (a)**

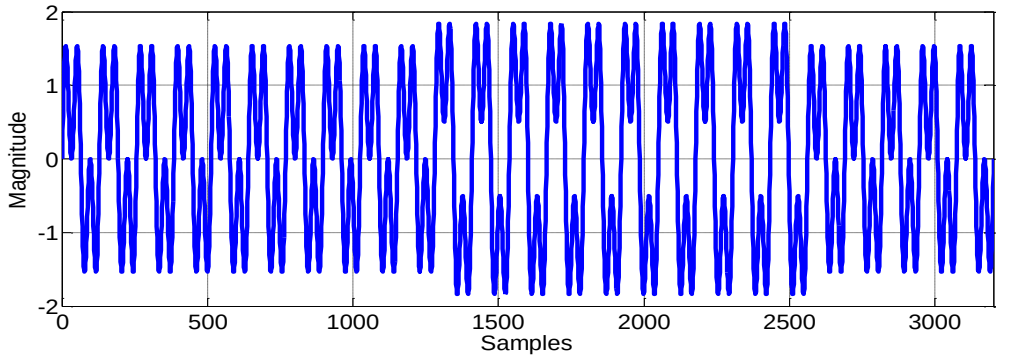


**Figure 2.8 (b)**

**Figure 2.8 (a) and (b) Voltage Swell with 3rd Harmonic**

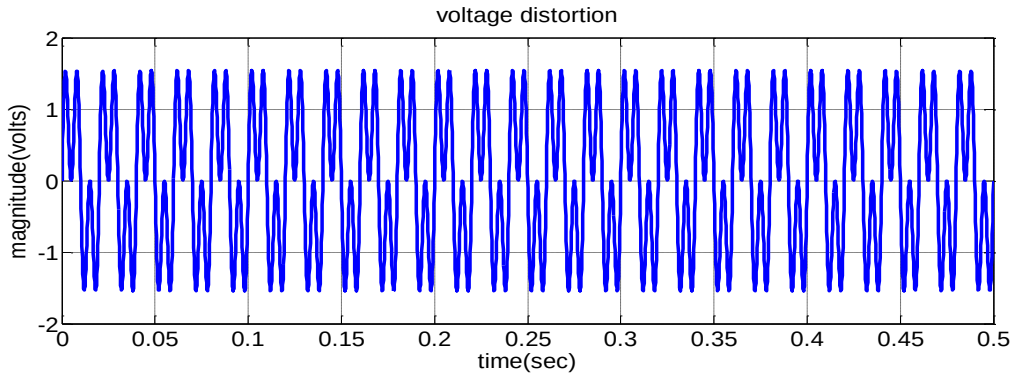


**Figure 2.9 (a)**

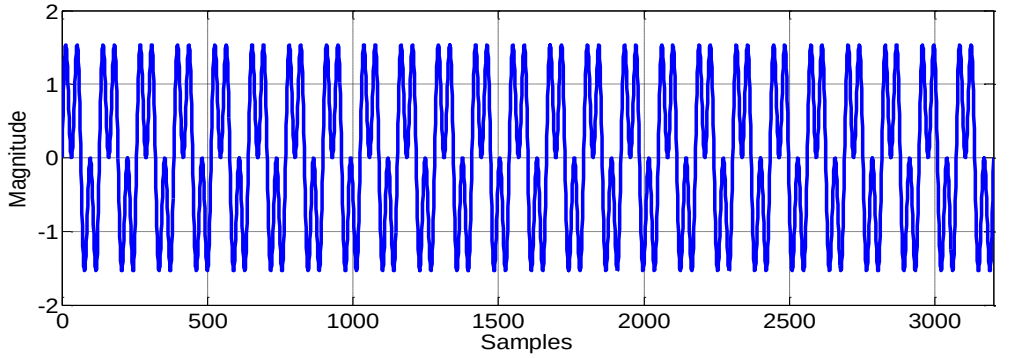


**Figure 2.9 (b)**

**Figure 2.9 (a) and (b) Voltage distortion**

## 2.4 Detection using WT

The above Disturbances are decomposed into different levels through wavelet decomposition algorithm as shown in Figure 2.1 using equation 2.1 and equation 2.2.The signal is looked at different scales or resolution which is also known as multi resolution analysis(MRA) or sub band coding. With increase in each level time resolution decreases while frequency resolution increases. The unique deviation of each power quality disturbances from the original sinusoidal waveform is identified both in the approximate and detail coefficients. The different disturbances are studied with different levels. Normally, one or two scale signal decomposition is adequate to discriminate disturbances from their background because the decomposed signals at lower scales have high time localization. In other words, the high scale signal decomposition is not necessary since it gives poor time localization. In this case the different power quality disturbances are decomposed up to $4^{th}$ level for detection purpose.

### 2.4.1 Voltage Sag

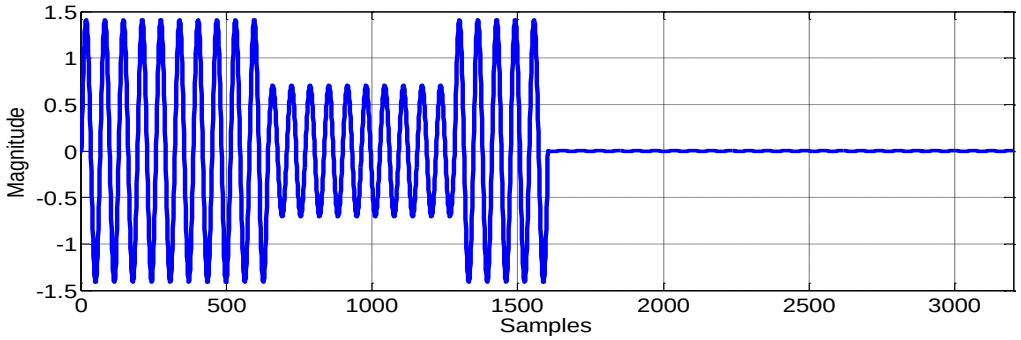


**Figure 2.10 (a) Decomposed voltage sag level 1 using WT**

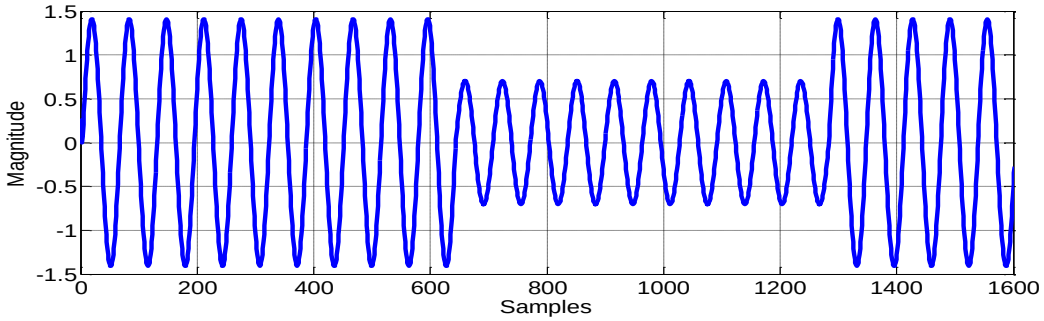


**Figure 2.10 (b) Approximate signal level 1**

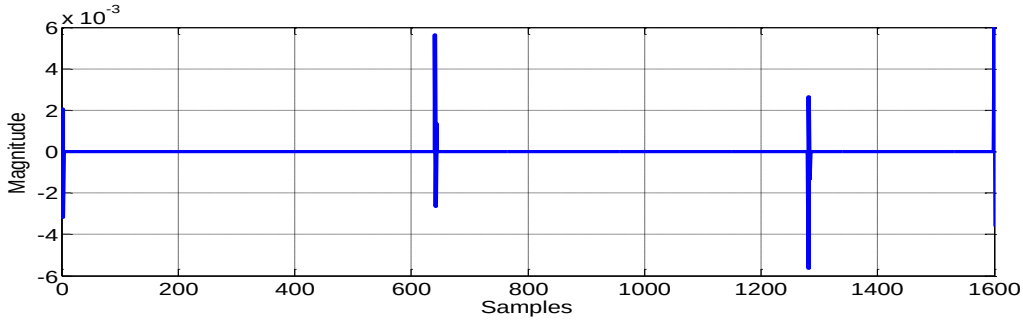


**Figure 2.10 (c) Detail signal level 1**

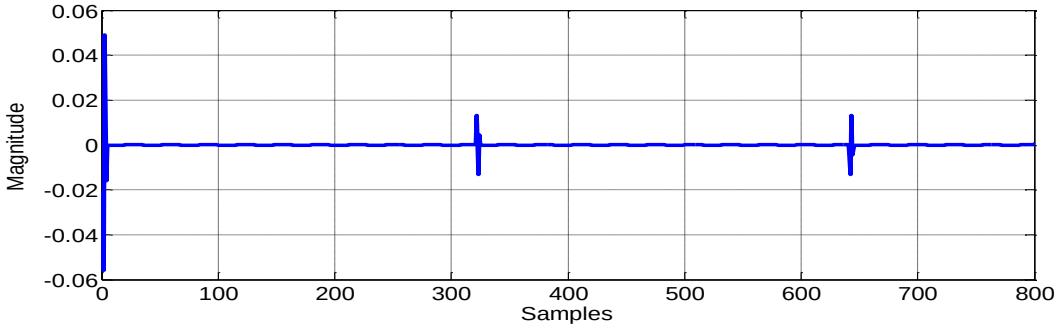


**Figure 2.10 (d) Detail signal level 2**

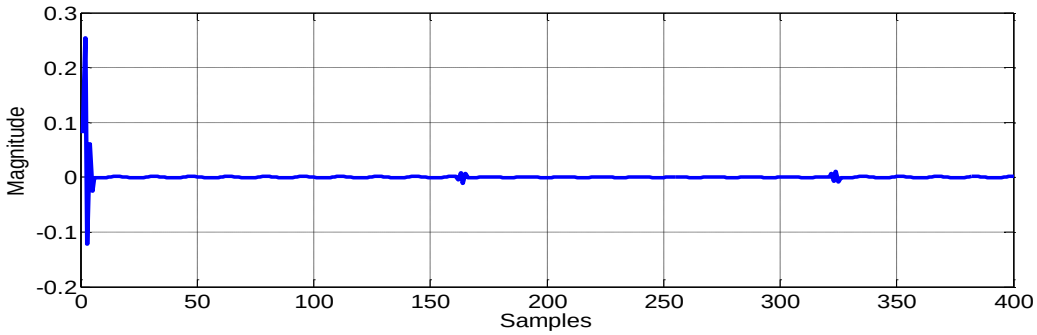


**Figure 2.10 (e) Detail signal level 3**

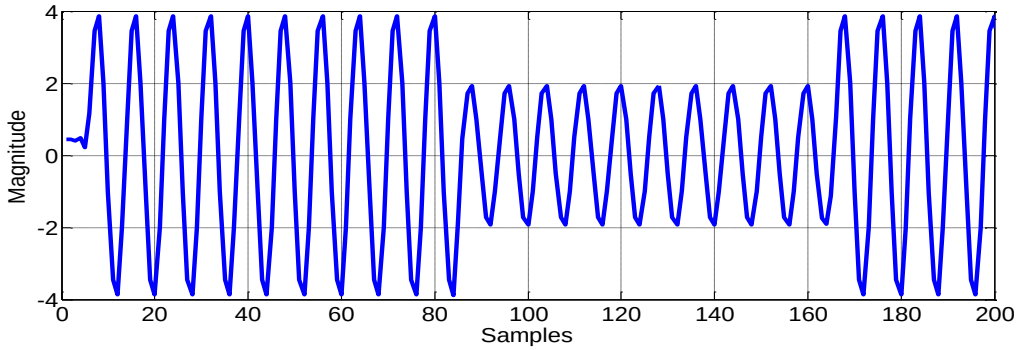


**Figure 2.10 (f) Approximate signal level 4**

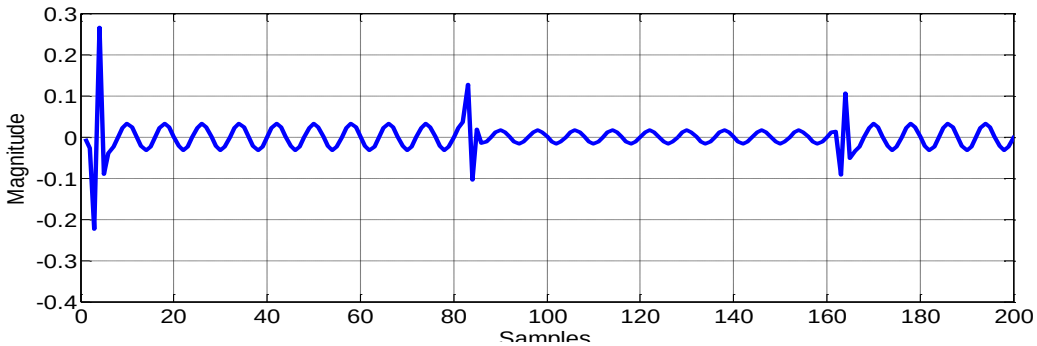


**Figure 2.10 (g) Detail signal level 4**

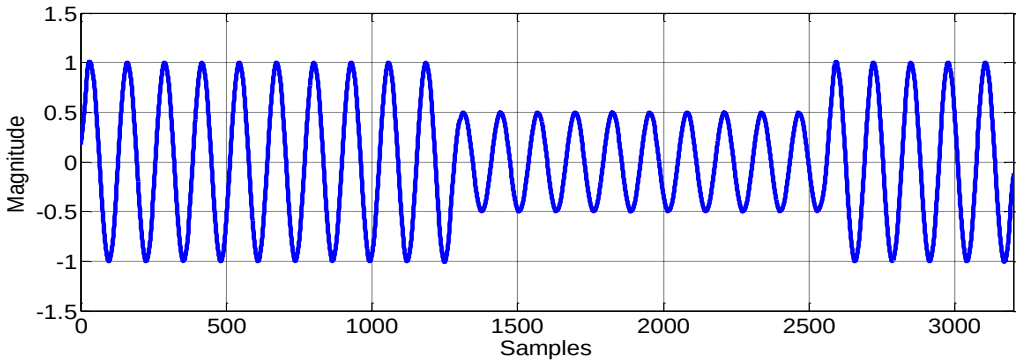


**Figure 2.10 (h) Reconstructed approximate signal**

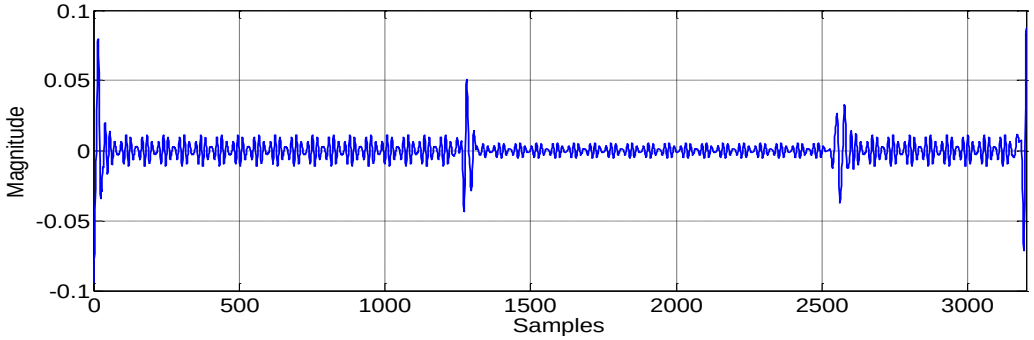


**Figure 2.10 (i) Reconstructed detail signal**

From the decomposition of the disturbance shown in Figure 2.4(a) and Figure 2.4(b) it is seen that disturbance occurred at 1250 to 2500 samples or 0.2 to 0.4 second interval of the signal which is confirmed from the result shown in Figure 2.10(h) and Figure 2.10(i).Reduction in nominal value of the waveform can be marked from the approximate and detail coefficient of level4 decomposition as shown in Figure 2.10(f) and Figure 2.10(g).The reconstructed approximate waveform shown in Figure 2.10(h) also perfectly resembles with input disturbance waveform shown in Figure 2.4(b) which confirmed the disturbance to be the voltage Sag and proves the accurate detection of the disturbance.

### 2.4.2 Voltage Swell

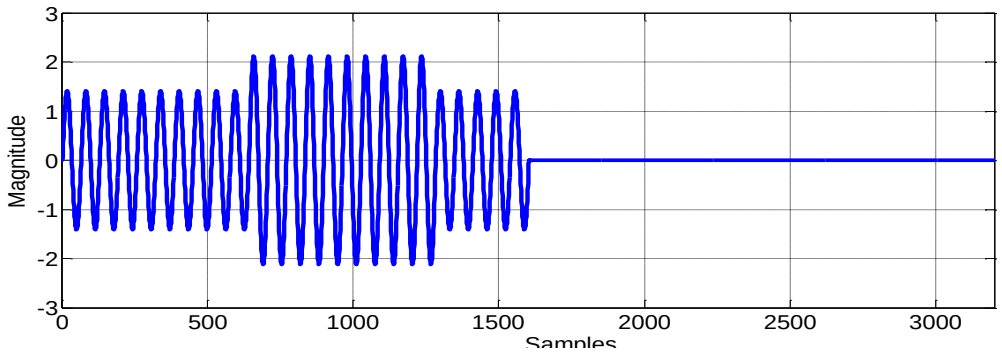


**Figure 2.11 (a) Decomposed voltage swell using WT**

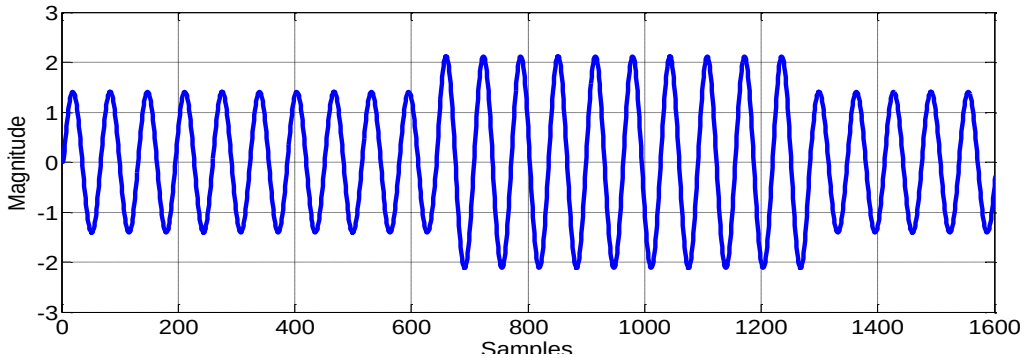


**Figure 2.11 (b) Approximate signal level 1**

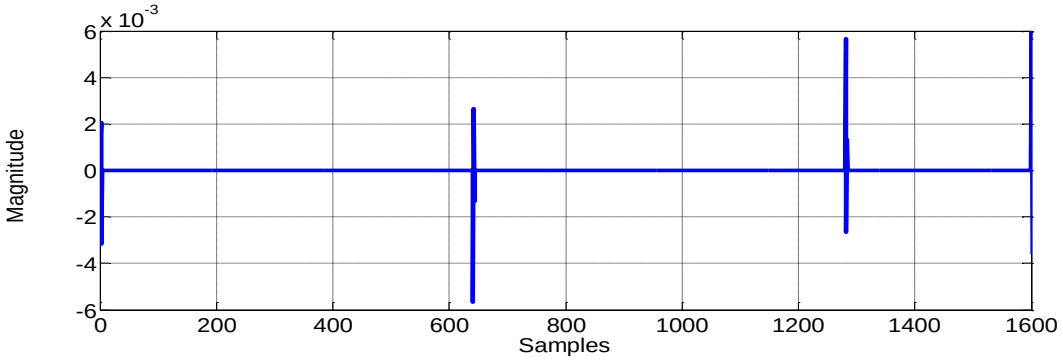


**Figure 2.11 (c) Detail signal level 1**

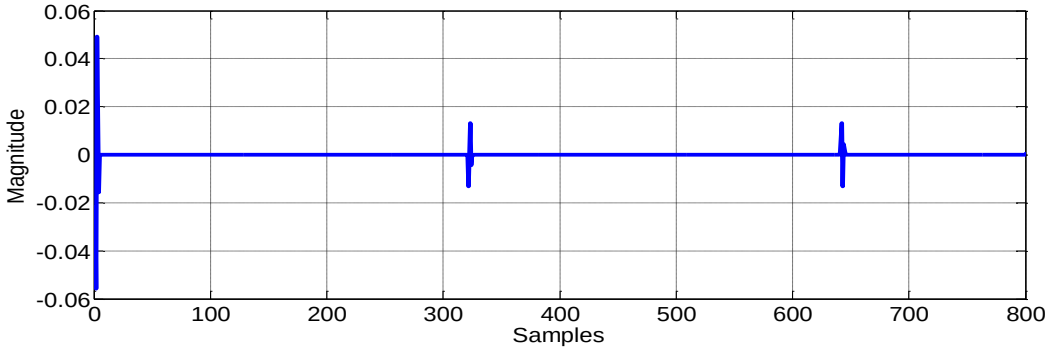


**Figure 2.11 (d) Detail signal level 2**

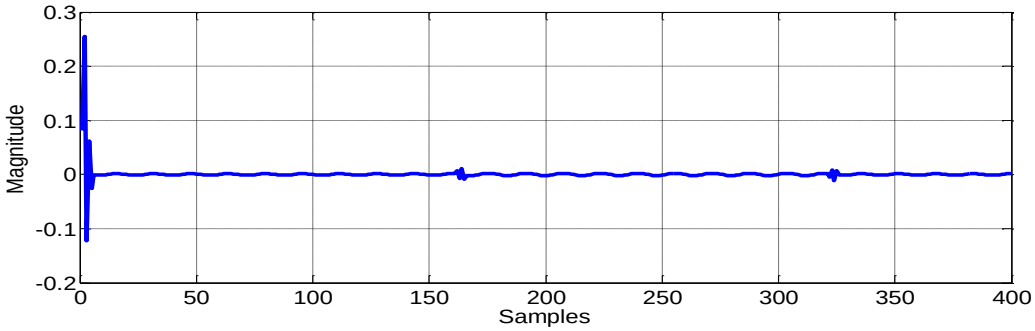


**Figure 2.11 (e) Detail signal level 3**

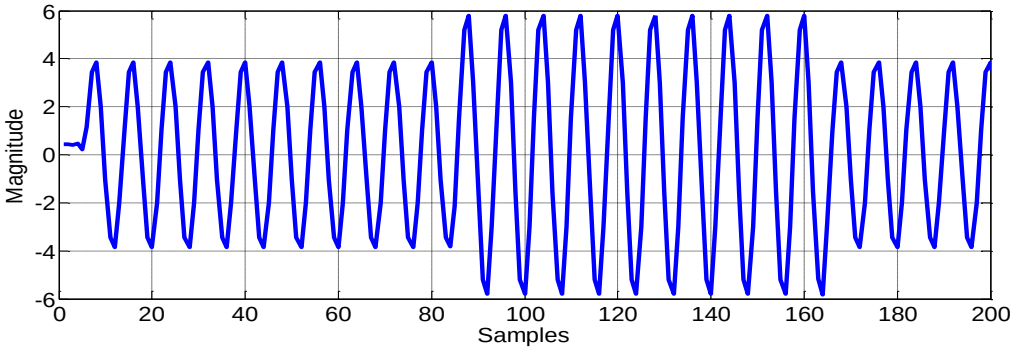


**Figure 2.11 (f) Approximate signal level 4**

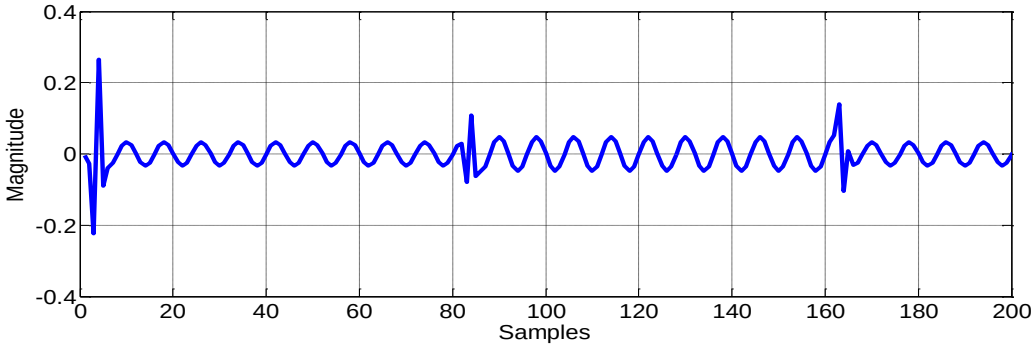


**Figure 2.11 (g) Detail signal level 4**

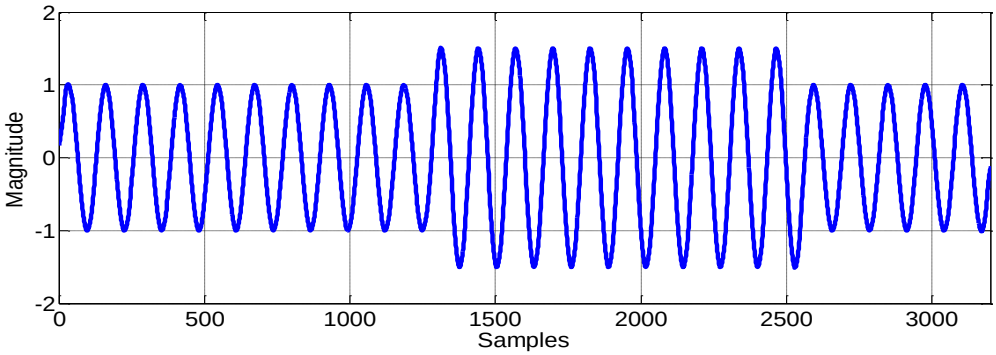


**Figure 2.11 (h) Reconstructed approximate signal**

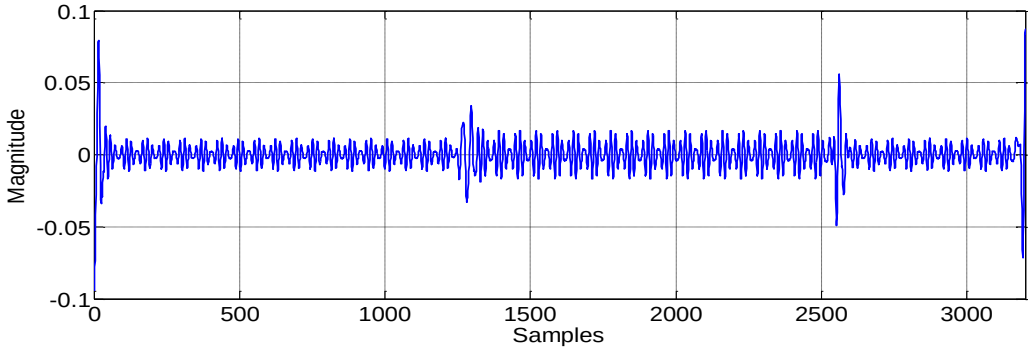


**Figure 2.11 (i) Reconstructed detail signal**

From the decomposition of the disturbance shown in Figure 2.5(a) and Figure 2.5(b) it is seen that disturbance occurred at 1250 to 2500 samples or 0.2 to 0.4 second interval of the signal which is confirmed from the result shown in Figure 2.11(h) and Figure 2.11(i).Increase in nominal value of the voltage at the disturbance instant can be marked from the approximate and detail coefficient of level4 decomposition as shown in Figure 2.11(f) and Figure 2.11(g).The reconstructed approximate waveform shown in Figure 2.11(h) also perfectly resembles with input disturbance waveform shown in Figure 2.5(b) which confirms the PQ disturbance to be Swell and proves the accurate detection of the disturbance.

### 2.4.3 Voltage interruption

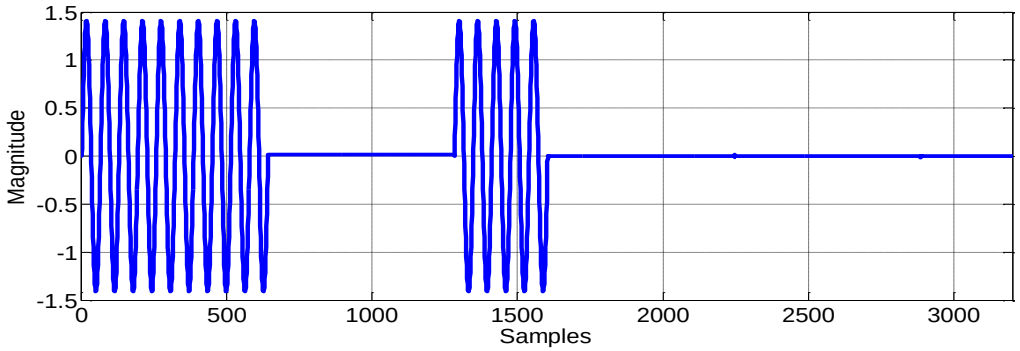


**Figure 2.12 (a) Decomposed voltage interruption using WT**

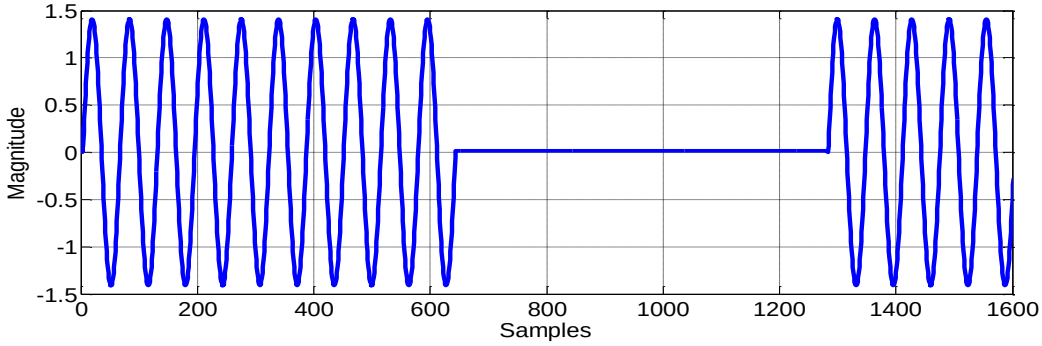


**Figure 2.12 (b) Approximate signal level 1**

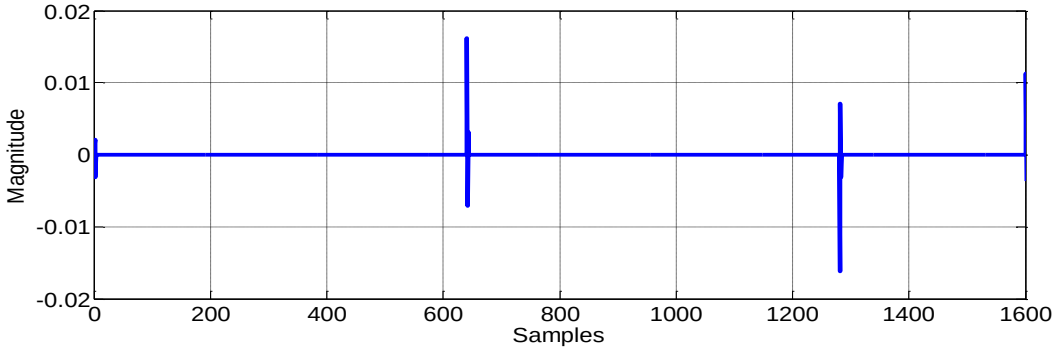


**Figure 2.12 (c) Detail signal level 1**

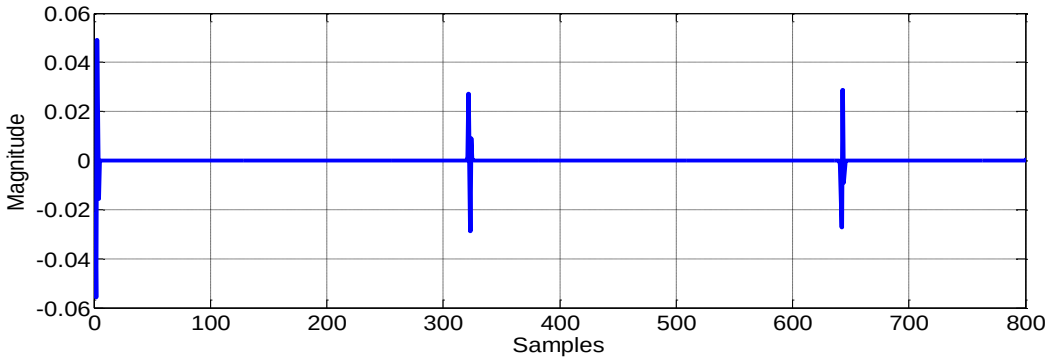


**Figure 2.12 (d) Detail signal level 2**

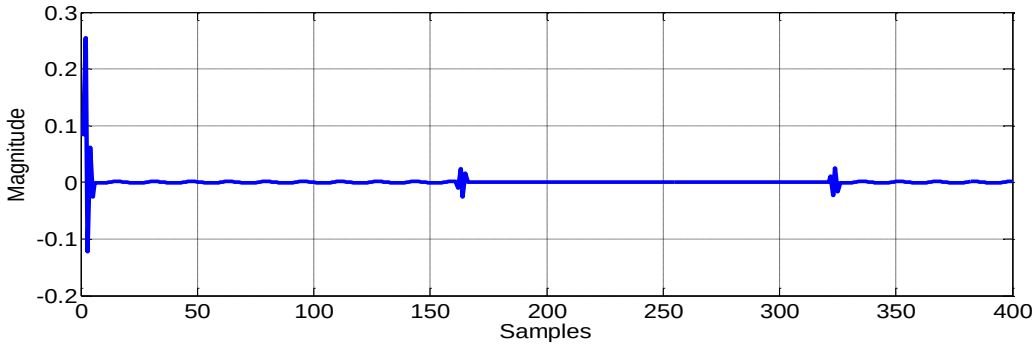


**Figure 2.12 (e) Detail signal level 3**

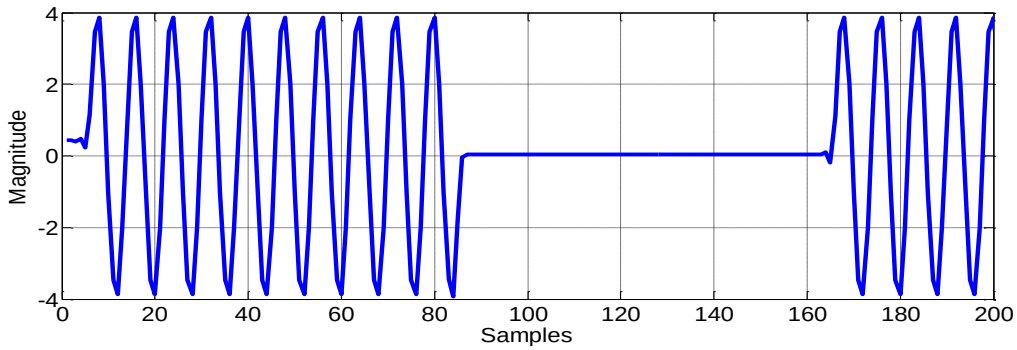


**Figure 2.12 (f) Approximate signal level 4**

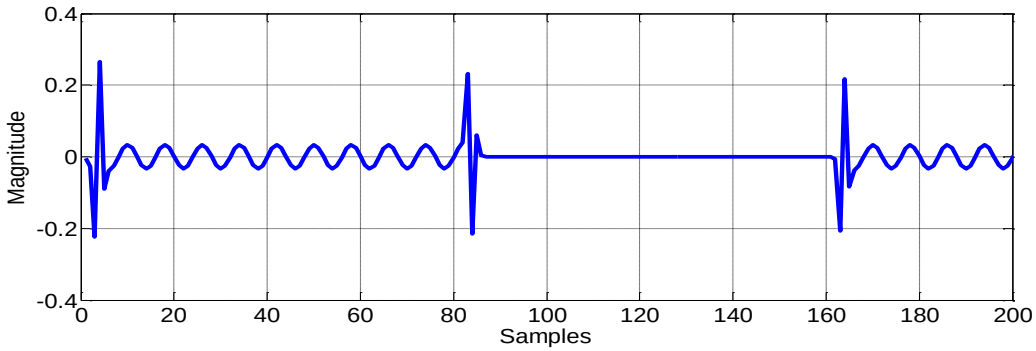


**Figure 2.12 (g) Detail signal level 4**

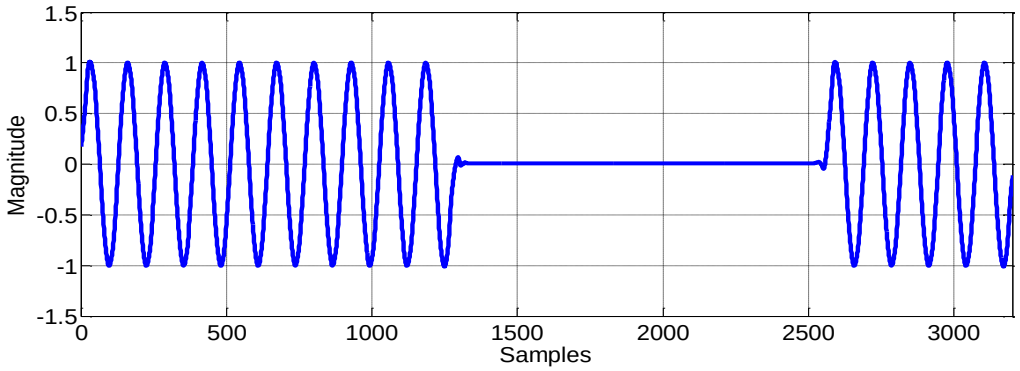


**Figure 2.12 (h) Reconstructed approximate signal**

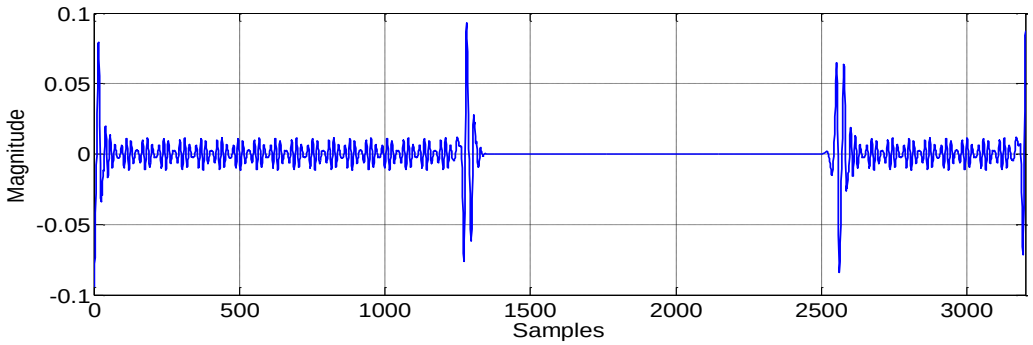


**Figure 2.12 (i) Reconstructed detail signal level 4**

From the decomposition of the disturbance shown in Figure 2.6(a) and Figure 2.6(b) it is seen that disturbance occurred at 1250 to 2500 samples or 0.2 to 0.4 second interval of the signal which is confirmed from the result shown in Figure 2.12(h) and Figure 2.12(i).The interruption in nominal value of the voltage at the disturbance instant can be marked from the approximate and detail coefficient of level4 decomposition as shown in Figure 2.12(f) and Figure 2.12(g).The reconstructed approximate waveform shown in Figure 2.12(h) also perfectly resembles with input disturbance waveform shown in Figure 2.6(b) which confirms the PQ disturbance to be Voltage interruption and proves the accurate detection of the disturbance.

### 2.4.4 Voltage Sag with harmonics

The complex disturbances like Sag with harmonics and Swell with harmonics can also be detected using wavelet decomposition algorithm similar to as discussed in case of voltage sag and voltage swell. Figure 2.13 shows the decomposition and detection of Sag with harmonics. Here only third harmonic component is added to the fundamental component of voltage sag to obtain the voltage sag with harmonics. Similarly other harmonic components can also be added and can be detected using WT.

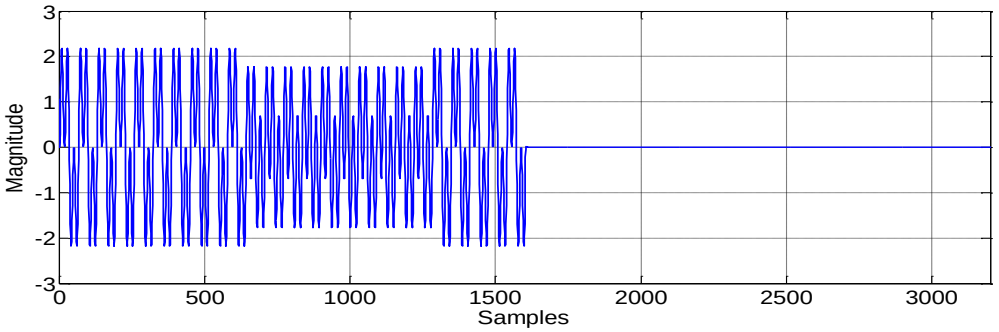


**Figure 2.13(a) Decomposed signal level 1 using WT**

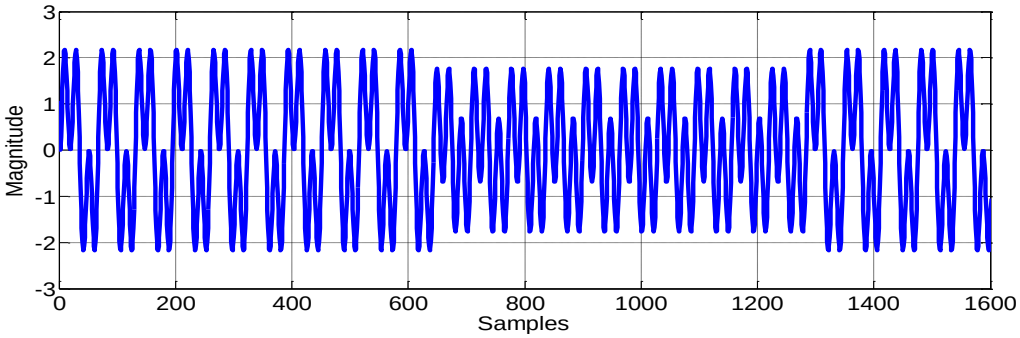


**Figure 2.13(b) Approximate signal level 1**

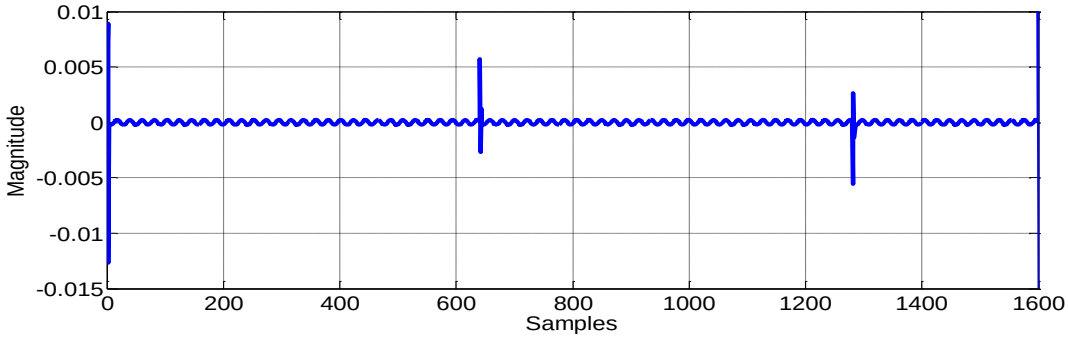


**Figure 2.13(c) Detail signal level 1**

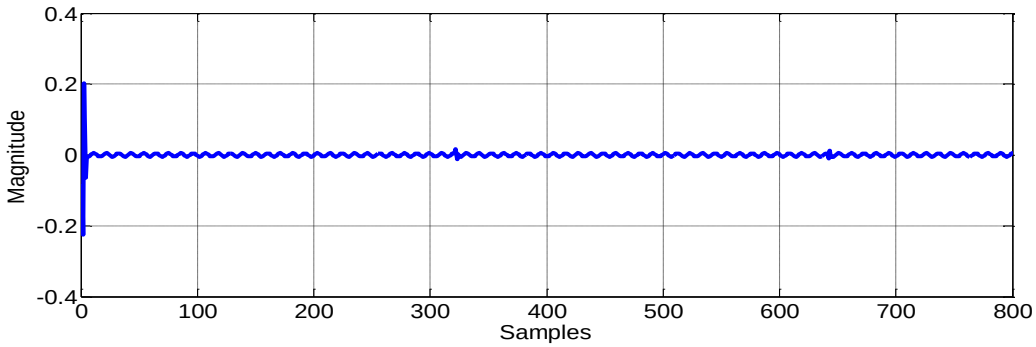


**Figure 2.13(d) Detail signal level 2**

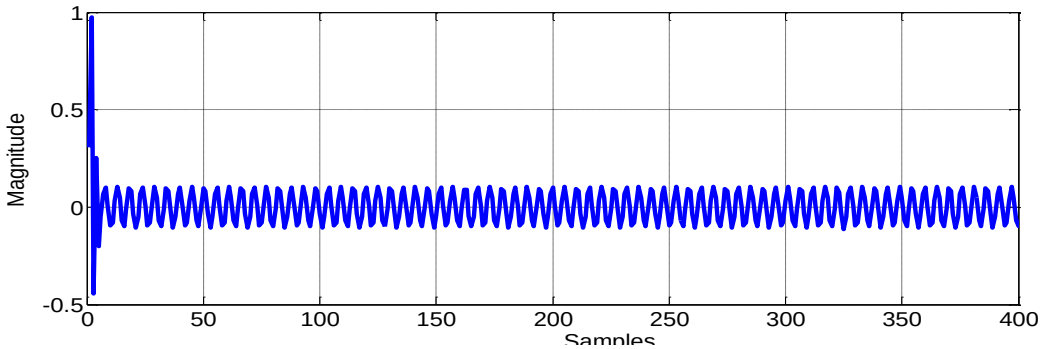


**Figure 2.13(e) Detail signal level 3**

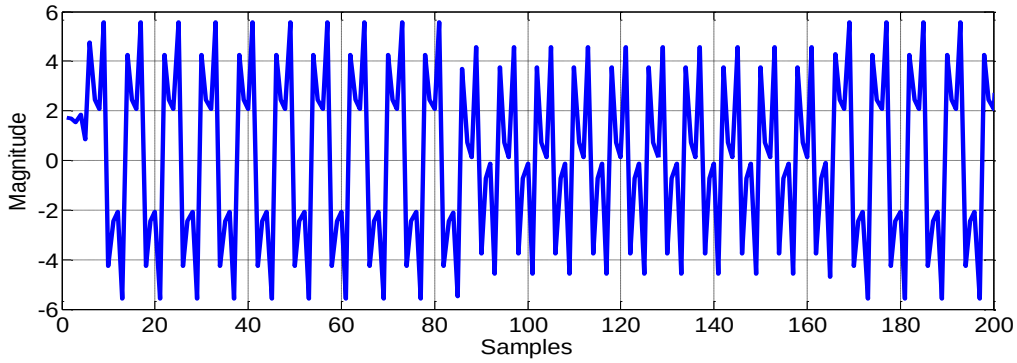


**Figure 2.13(f) Approximate signal level 3**

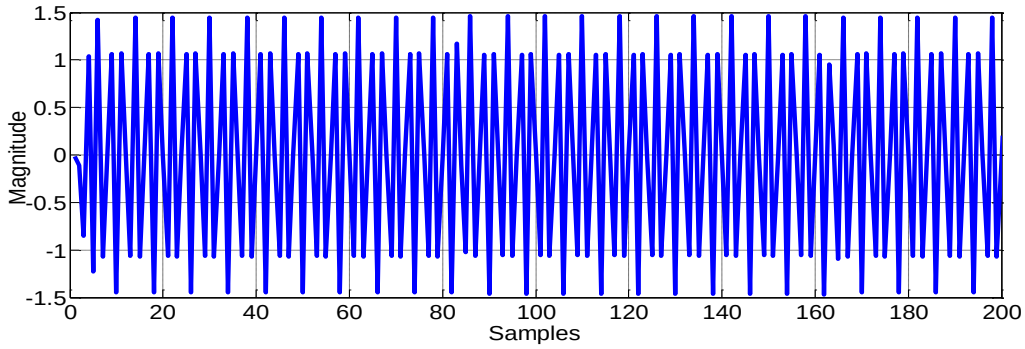


**Figure 2.13(g) Detail signal level 4**

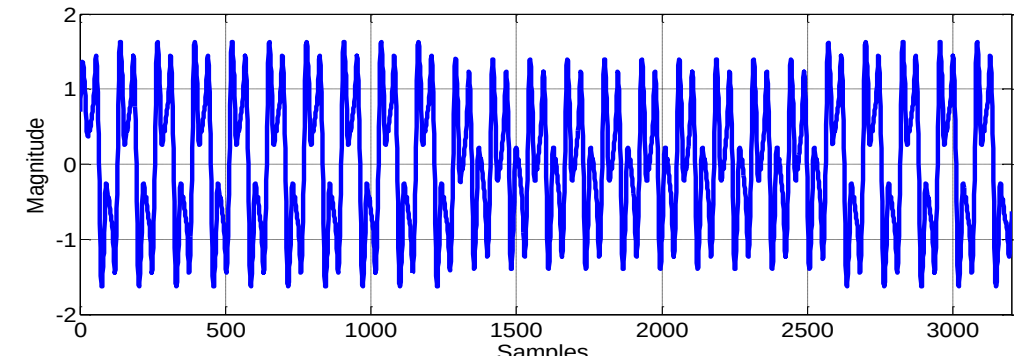


**Figure 2.13(h) Reconstructed approximate signal**

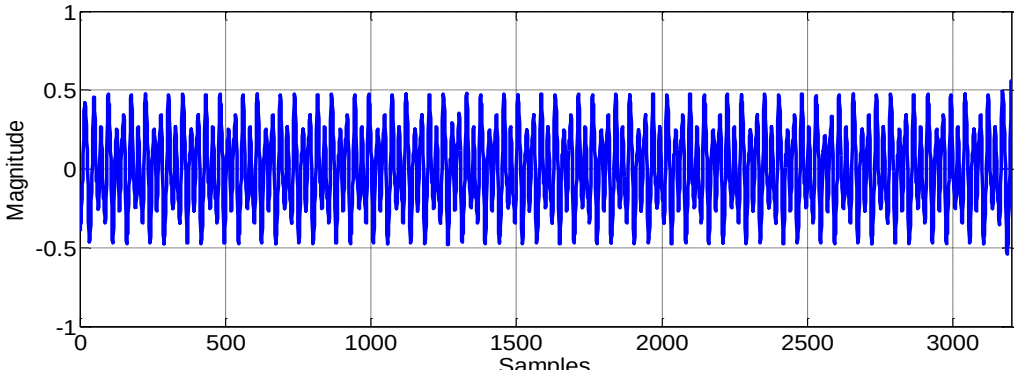


**Figure 2.13(i) Reconstructed detail signal**

From the Figure 2.13 (h) and Figure 2.13 (i) it is quite clear that the disturbance is Sag which contains harmonics. Reconstructed Approximate signal in Figure 2.13 (h) resembles with input disturbance shown in Figure 2.7 (b) which proves the detection is accurate and detail signal in Figure 2.13 (g) confirms that it contains harmonics.

### 2.4.5 Voltage swell with harmonics

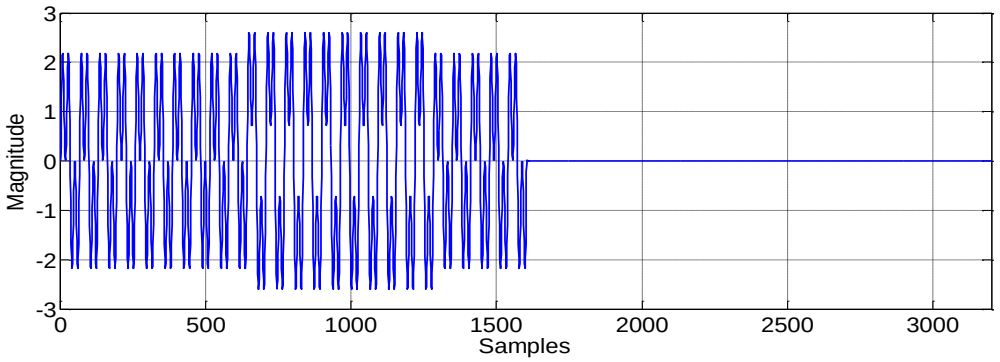


**Figure 2.14 (a) Decomposed signal level 1 using WT**

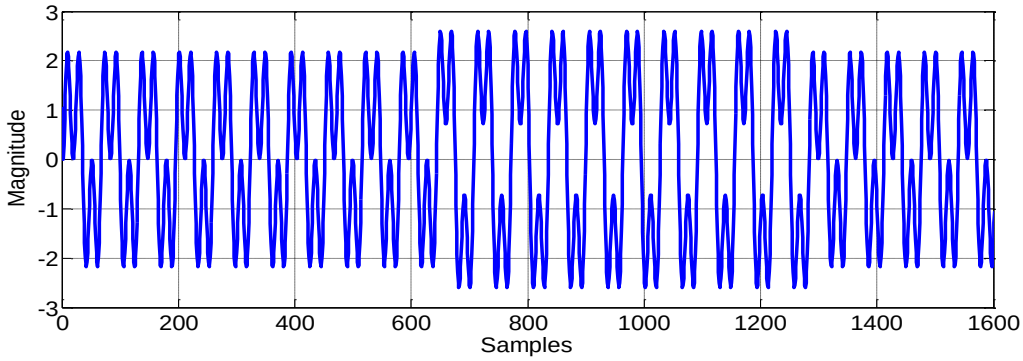


**Figure 2.14 (b) Approximate signal level 1**

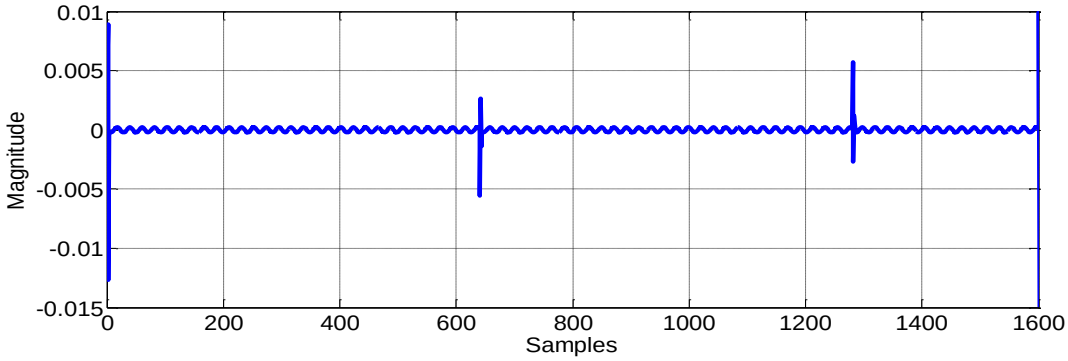


**Figure 2.14(c) Detail signal level 1**

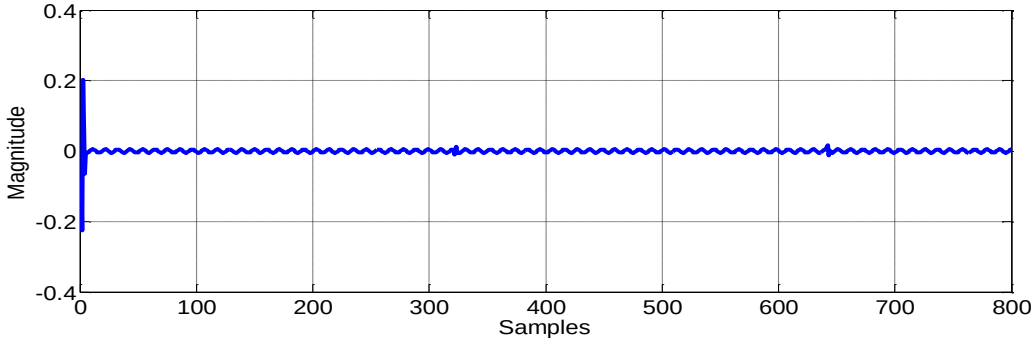


**Figure 2.14 (d) Detail signal level 2**

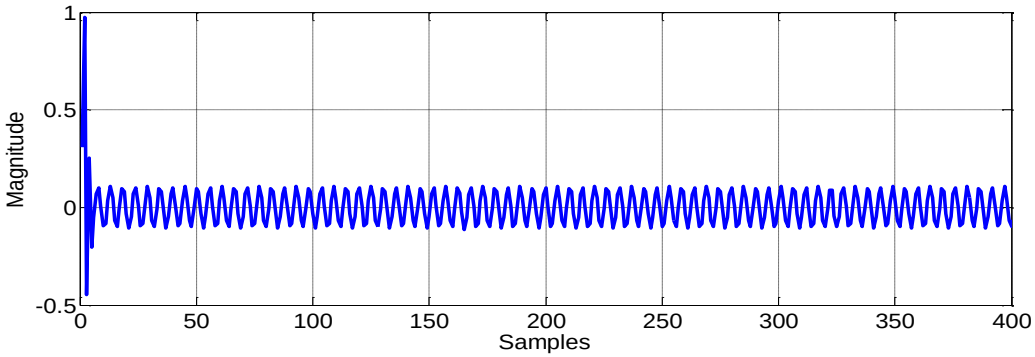


**Figure 2.14 (e) Detail signal level 3**

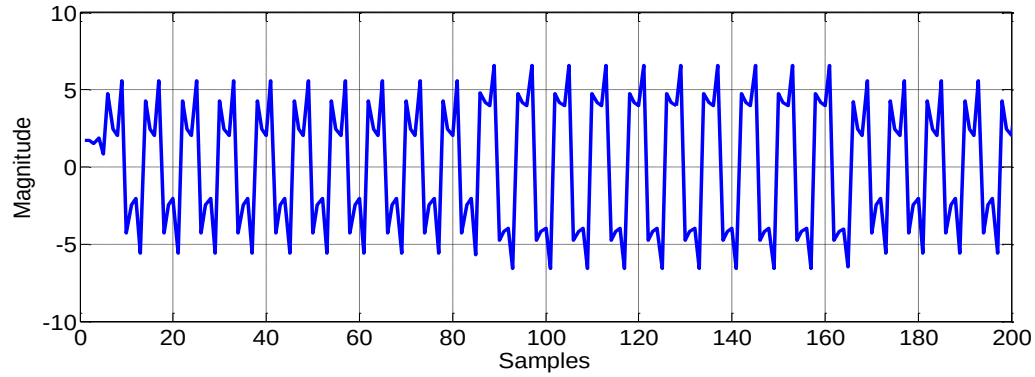


**Figure 2.14 (f) Approximate signal level 4**

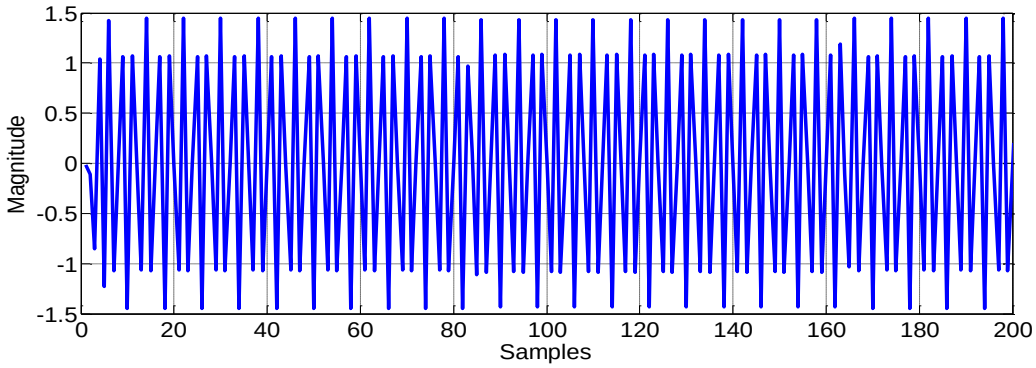


**Figure 2.14 (g) Detail signal level 4**

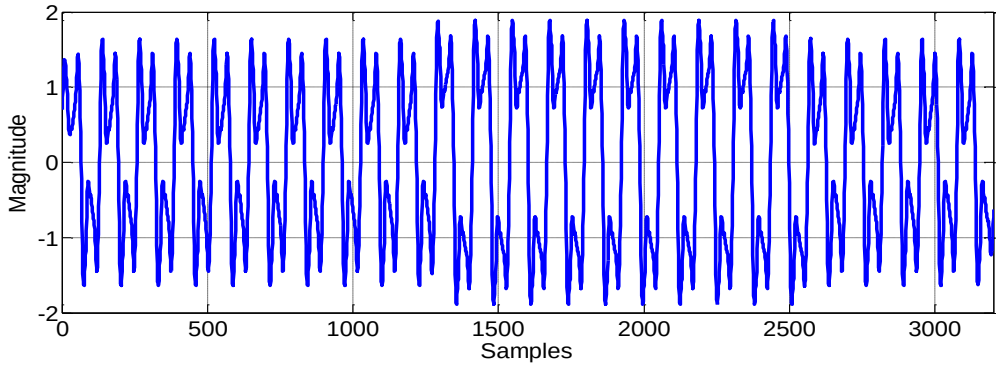


**Figure 2.14 (h) Reconstructed approximate signal**

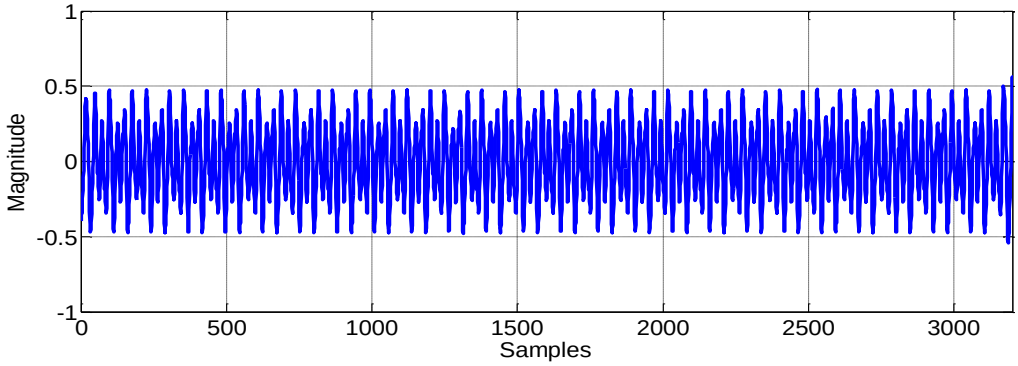


**Figure 2.14 (i) Reconstructed detail signal**

From the Figure 2.14 (h) and Figure 2.14 (i) it is quite clear that the disturbance is Swell which contains harmonics. Approximate signal in Figure 2.14 (h) resembles with input disturbance shown in Figure 2.8 (b) which proves the detection is accurate and detail signal in Figure 2.14 (g) confirms that it contains harmonics.

## 2.5 Detection in presence of noise

The presence of noise in power quality disturbances creates a new challenge for detection as it is difficult to detect the exact location of disturbance in a high noisy environment with a low SNR(signal to noise ratio).The Presence of noise also affects the classification accuracy as the feature vectors to be extracted for classification will also contain the noise contribution and the exact quantity of noise present is quite uncertain and hence de-noising of the disturbance is necessary before feature extraction and classification. In this work the white Gaussian noise is added to the pure power quality disturbances as shown in Figure 2.4, Figure 2.5 and Figure 2.6 to simulate a low SNR of 5 dB.The white Gaussian noise added to different PQ disturbances is shown in Figure 2.15.

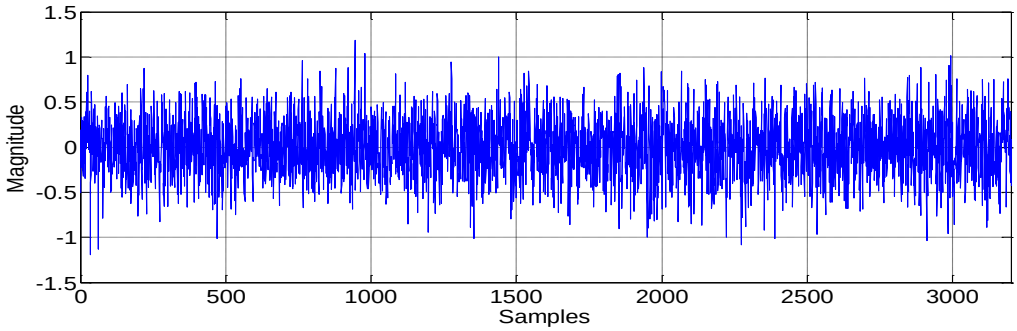


**Figure 2.15 Additive white Gaussian noise**

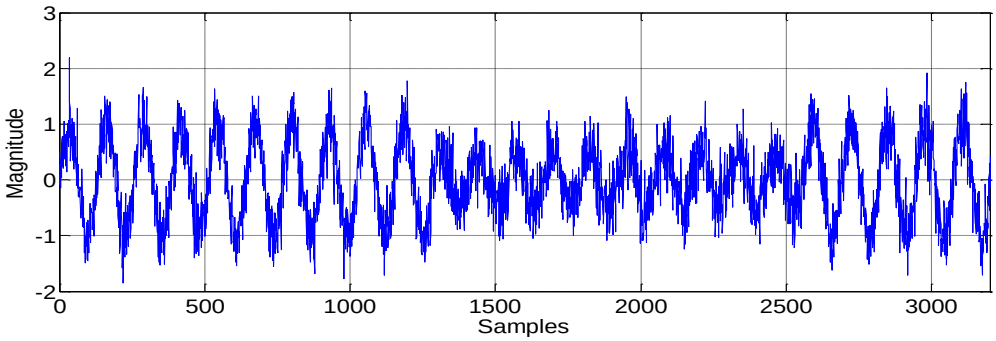


**Figure 2.16 Sag polluted with noise**

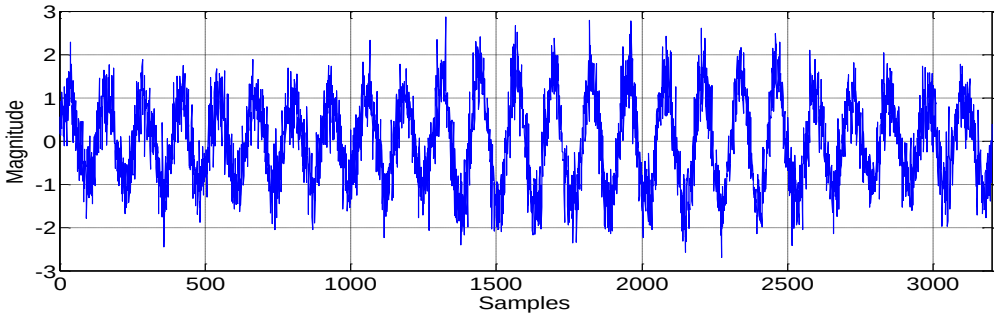


**Figure 2.17 Swell polluted with noise**

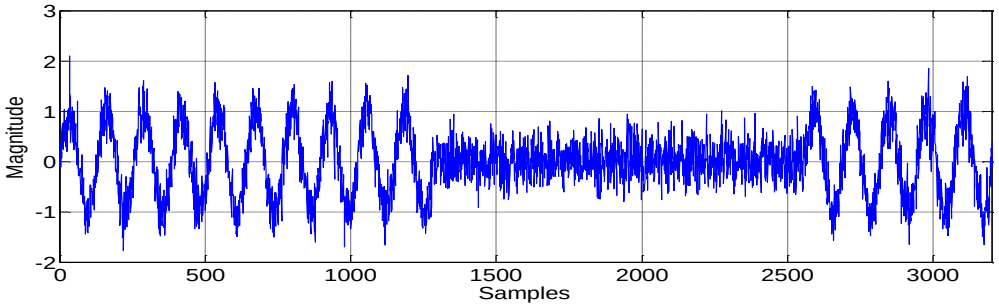


**Figure 2.18 Interruption with noise**

### 2.5.1 Difficulty in Detection in presence of noise

In the presence of noise, the localisation of disturbance is quite difficult which is shown below in Figure 2.19 in the case of Sag disturbance corrupted with noise. From the results obtained it is clearly observed that even after decomposing the disturbance into several levels the exact location of disturbance cannot be identified in terms of the detail coefficient of the disturbance which was easily identified in case of the disturbance without noise.

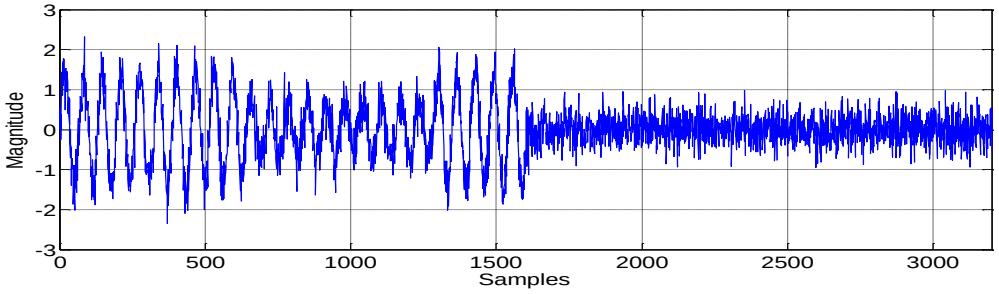


**Figure 2.19 (a) Decomposed Sag with noise using WT**

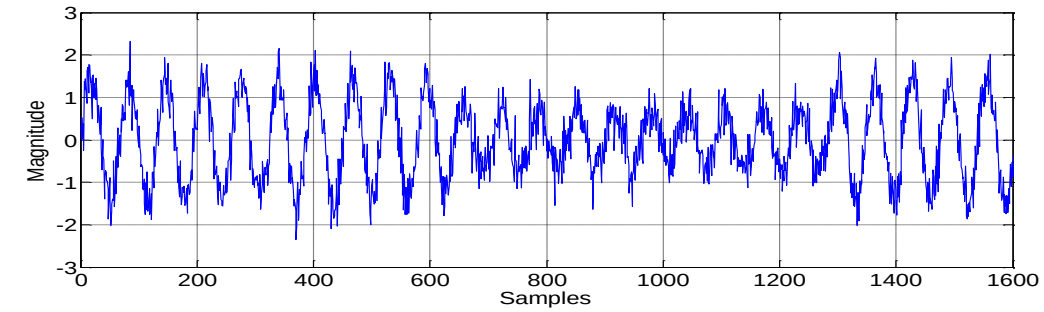


**Figure 2.19 (b) Approximate signal level 1**

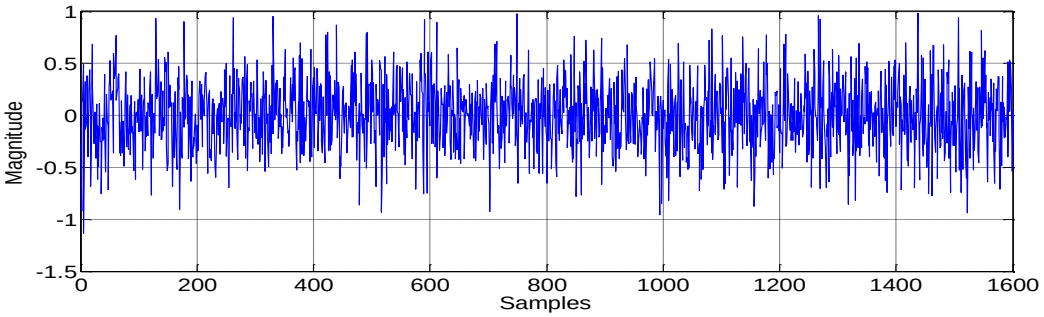


**Figure 2.19 (c) Detail Signal Level 1**

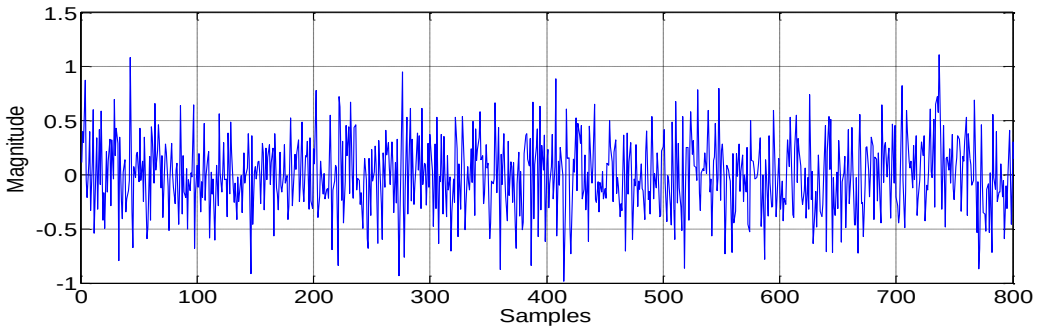


**Figure 2.19 (d) Detail Signal Level 2**

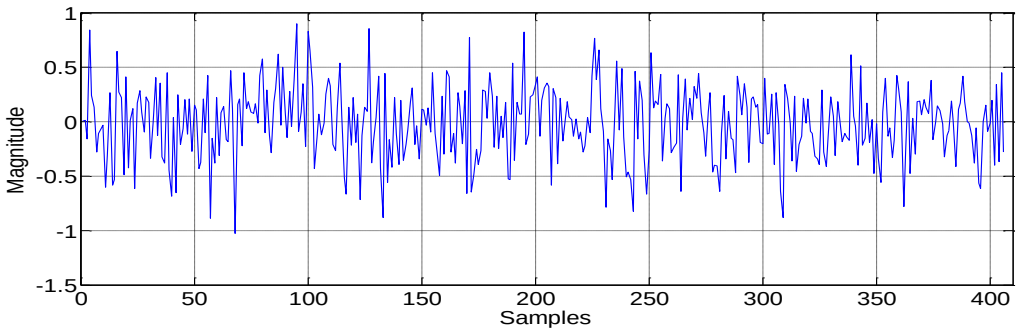


**Figure 2.19 (e) Detail Signal Level 3**

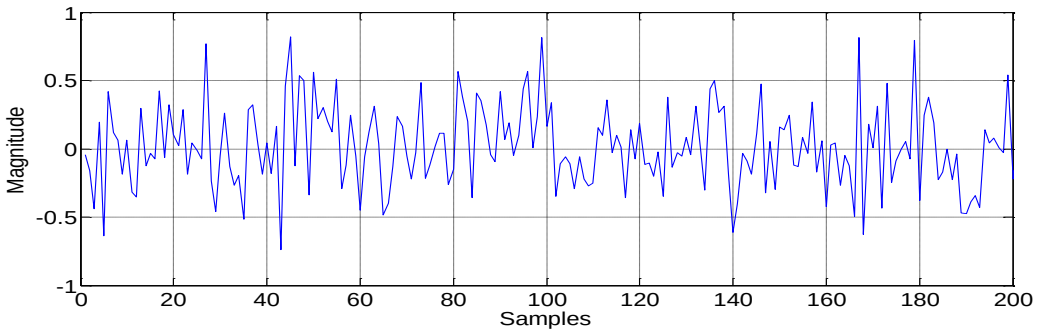


**Figure 2.19 (f) Detail Signal Level 4**

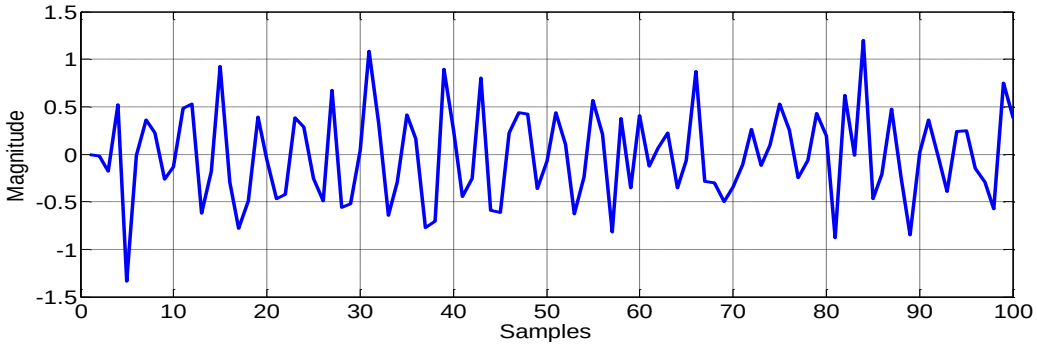


**Figure 2.19 (g) Detail Signal Level 5**

From the results shown in Figure 2.19 it is quite clear that in spite of decomposing the disturbance corrupted with noise into several levels accurate localisation of disturbing instant cannot be obtained in terms of detail coefficients as shown in Figure 2.19 (c),(d),(e),(f)and (g). These conditions are not ideal for the detection of the disturbances as well as for the feature extraction as it contains a high percentage of noise which may degrade the classification accuracy.

## 2.6 Summary

From the decomposition results obtained in this work it is quite evident that the Wavelet transform as a tool for detecting PQ disturbances works very well and can be employed effectively in designing a monitoring system for power quality events. Here different PQ disturbances like sag, swell, interruption, and some complex disturbances like sag with harmonics and swell with harmonics are decomposed into several levels and correctly located the point of disturbance. The problem occurs when the disturbances are corrupted with noise, accurate localisation of disturbing instant is difficult in terms of the detail coefficients. Hence in presence of noise direct decomposition of the disturbances with WT is not sufficient, so de-noising of disturbances is necessary before feature extraction and classification otherwise the classification accuracy is going to decrease as the feature vector to be extracted will

contain a high percentage of noise. Hence de-noising is very much necessary. A de-noising technique is discussed in the next chapter.

## 3.1 Introduction

The proper detection i.e. the critical start-time and end-time of power quality (PQ) disturbances is an important aspect in monitoring and locating of the fault instances so as to extract the features and develop a classification system but the signal under investigation is often polluted by noises, rendering the extraction of features a difficult task, especially if the noises have high frequency spectrum which overlaps with the frequency of the disturbances. The performance of the classification system would be greatly degraded, due to the difficulty in distinguishing the noises and the disturbances and also the feature vector to be extracted will contain noise. Hence it is an important application of wavelet analysis in power system to de-noise power quality signals so as to detect and locate the disturbing points as the presence of noise in power quality events may degrade the classification accuracy.In this chapter a wavelet based de-noising technique is discussed based on soft thresholding so as to de-noise the PQ disturbances and improve the performance of classification system.

## 3.2 De-nosing using WT

### 3.2.1 Steps involved in De-noising

Basically there are 3 steps involved in de-noising process which is mentioned below.

Decomposition: This step involves selecting a proper mother wavelet and choosing a level *n* up to which the signal *S* is decomposed using the selected mother wavelet. The mother wavelet selected in this work is “db4” as it gives good results in dealing with PQ disturbances. The level of decomposition *n* is selected as per the requirement and in this case it is chosen five.

Detail coefficients Thresholding: For each level from 1 to *n*, a threshold is selected and soft thresholding is applied to the detailed coefficients.

Reconstruction: Wavelet reconstruction is computed based on the original approximation coefficients of level *n* and the modified detail coefficients of levels from 1 to *n*.

### 3.2.2 Thresholding based De-noising

In the first stage, the polluted sinusoidal signal is decomposed by selected wavelet basic function “Db4” to certain level, here up to 5 levels. Coefficients at each level are compared within this level and absolute maximum coefficient will be stored to be the threshold value at this level. The maximum coefficient is selected as it represents the maximum noise characteristic. Any coefficients higher than this value are totally noise unrelated, and are thus only possibly associated with power quality disturbance. After computation, five detailed

threshold values and one approximate threshold value will be stored for future signal de-noising. In the second stage, the power quality disturbance signals polluted by noises are recorded as before. The disturbance signal is decomposed by the same wavelet basic function to the same level to generate wavelet transform coefficients. All the coefficients at each level will be thresholded by the corresponding threshold value that is determined by the previous stage. All those threshold values represent the maximum noise characteristics. Any coefficients after the thresholding are the disturbance coefficients. Therefore after decomposition, the coefficients of the signal are greater than the coefficients of the noise, so we can find a suitable T as a threshold value. When the wavelet coefficient is smaller than the threshold, it is considered that the wavelet coefficient is mainly caused by the noise, so that the coefficient is set to 0,and then discarded; When the wavelet coefficient is larger than the threshold, it is considered that wavelet coefficient is mainly caused by the signal, so that the coefficient is remained or shrinks to zero according to a fixed value, and then the signal de-noised can be reconstructed through the new wavelet coefficients using wavelet transform. The method can be modelled as shown below in (3.1).

$$S(n) = X(n) + \varepsilon.e(n) \tag{3.1}$$

*Where n=0,1,2…k-1*

*S(n)* =Noisy Signal

*X(n)*=Useful Power Quality disturbance without noise

*e(n)*=The noise added to *X(n)*

### 3.2.3 Selection of Thresholding function

The thresholding on the DWT coefficients during wavelet based de-noising methods can be performed using either hard or soft Thresholding. The hard threshold method is ineffective, and Hard threshold function is not continuous, thus it is mathematically difficult to deal with, and also has some discontinuity points, while de-noising. The Soft threshold function is continuous, thus it is better to overcome the shortcomings of the Hard Thresholding but the soft threshold method transforms so smooth that transition of PQ signal is distorted and this method reduces the absolute value of the large wavelet factor, causing a certain amount of high-frequency loss of information and the result leads to edge blur of the signal. However the soft thresholding is best suited for de-noising of PQ disturbances.

Soft Thresholding

$$d_n{}^j = \begin{cases} d_n{}^j & |d_n{}^j| \geq \lambda_j \\ 0 & |d_n{}^j| < \lambda_j \end{cases} \quad (3.2)$$

Hard Thresholding

$$d_n{}^j = \begin{cases} sign(d_n{}^j)(d_n{}^j - T) & |d_n{}^j| \geq \lambda_j \\ 0 & |d_n{}^j| < \lambda_j \end{cases} \quad (3.3)$$

Where $d_n{}^j$ =Detail Coefficient at level n and scale j

$\lambda_j$= Thresholding Value.

### 3.2.4 Selection of Thresholding rule

The selection of threshold value is crucial in wavelet based PQ signal de-noising. The careful rejection of the coefficients representing noise improves the accuracy of the de-noising results. Threshold $\lambda_j$ is decisive to de-noising effect, and the common threshold selection rules present in MATLAB are: sqtwolog, rigrsure, heursure and minimaxi.

**Rigrsure:** 'rigrsure' uses for the soft threshold estimator, a threshold selection rule based on Stein's Unbiased Estimate of Risk (quadratic loss function). One gets an estimate of the risk for a particular threshold value (t). Minimizing the risks in (t) gives a selection of the threshold value.

**Sqtwolog:** 'sqtwolog' uses a fixed-form threshold yielding minimax performance multiplied by a small factor proportional to log (length(X)).

**Heursure:** 'heursure' is a mixture of the two previous options. As a result, if the signal to noise ratio is very small, the SURE estimate is very noisy. If such a situation is detected, the fixed form threshold is used.

**Minimaxi:** 'minimaxi' uses a fixed threshold chosen to yield minimax performance for mean sqare error against an ideal procedure. The minimax principle is used in statistics in order to design estimators. Since the de-noised signal can be assimilated to the estimator of the

unknown regression function, the minimax estimator is the one that realizes the minimum of the maximum mean square error obtained for the worst function in a given set.

All the above rules employed a common thresholding formula which is also known as automatic thresholding rule.

$$\lambda_j = \frac{m_j}{0.6745}\left(\sqrt{2log_e(n_j)}\right) \tag{3.4}$$

Where $\lambda_j$ =Threshold value at scale j

$m_j$= Median value of Signal at scale j

$n_j$ = No of Coefficient at scale j

## 3.3 Results and discussion

The de-noising of Power Quality disturbances is performed using automatic Thresholding method as explained in 3.2.2 by selecting a threshold value for each level and Thresholding the detail coefficient and finally reconstructing the signal with modified detail coefficient and original approximate coefficient.

### 3.3.1 De-noising of sag disturbance

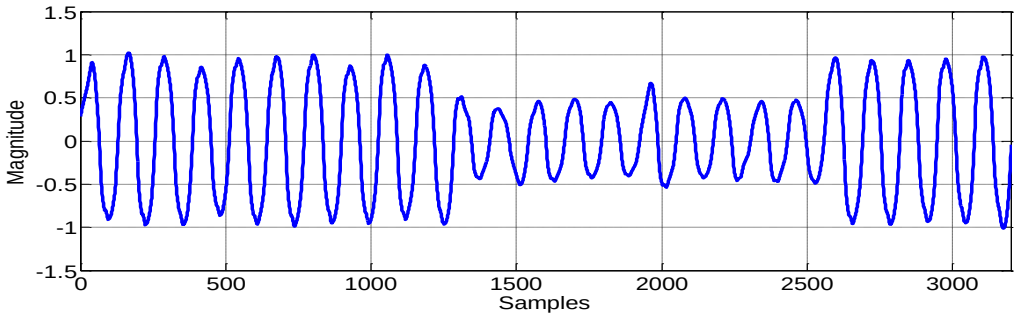


**Figure 3.1 (a) De-noised sag disturbance**

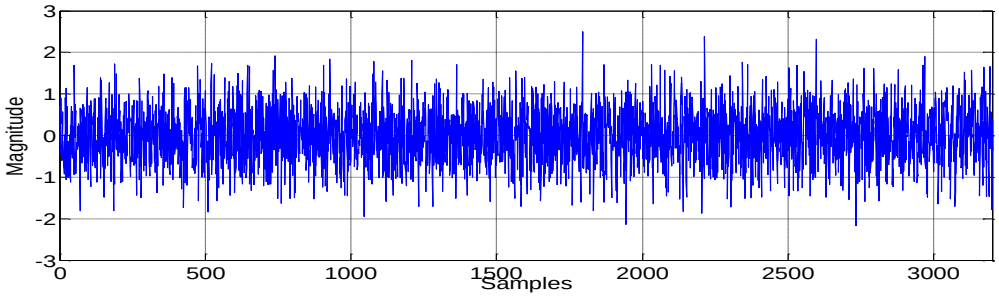


**Figure 3.1 (b) Amount of noise cleared**

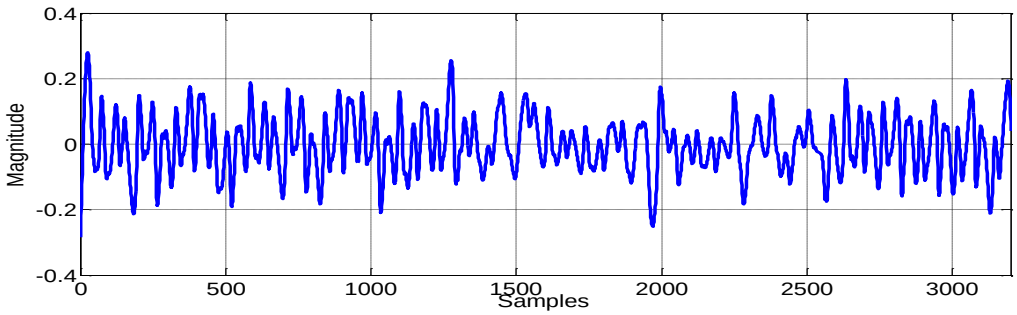


**Figure 3.1 (c) Residue after de-noising**

Figure 3.1 (a) is the de-noised Sag disturbance obtained after the implementation of the de-noising technique mentioned above in section 3.2.2. Figure 3.1(b) shows the amount of noise cleared which is obtained by subtracting the de-noised signal shown in Figure 3.1(a) from the noisy disturbance shown in Figure 2.16 in previous chapter.Figure 3.1(c) shows the residue after de-noising which is obtained by subtracting the de-noised signal obtained in Figure 3.1(a) from the Sag disturbance shown in Figure 2.4(b) in previous chapter.

### 3.3.2 De-noising of swell disturbance

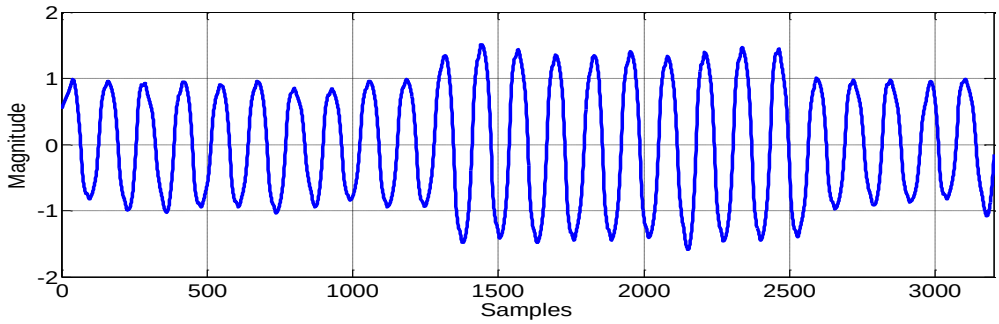


**Figure 3.2 (a) De-noised swell disturbance**

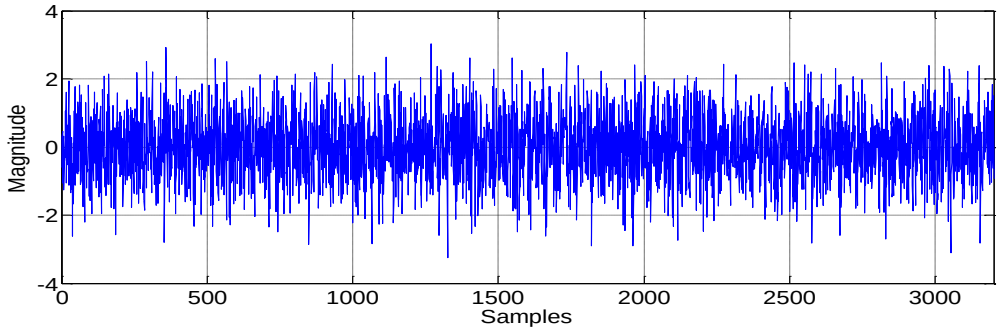


**Figure 3.2 (b) Amount of noise cleared**

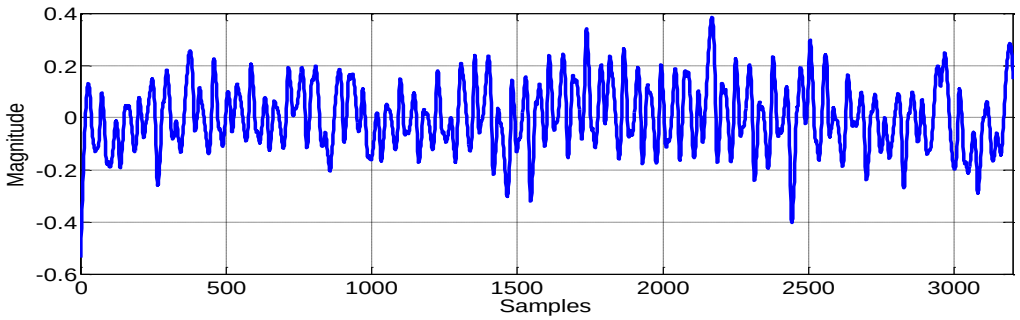


**Figure 3.2 (c) Residue after de-noising**

Figure 3.2 (a) is the de-noised Sag disturbance obtained after the implementation of the de-noising technique mentioned above in section 3.2.2. Figure 3.2(b) shows the amount of noise cleared which is obtained by subtracting the de-noised signal shown in Figure 3.2(a) from the noisy disturbance shown in Figure 2.17 in previous chapter.Figure 3.2(c) shows the residue after de-noising which is obtained by subtracting the de-noised signal obtained in Figure 3.2(a) from the Swell disturbance shown in Figure 2.5(b) in previous chapter.

### 3.3.3 De-noising of interruption disturbance

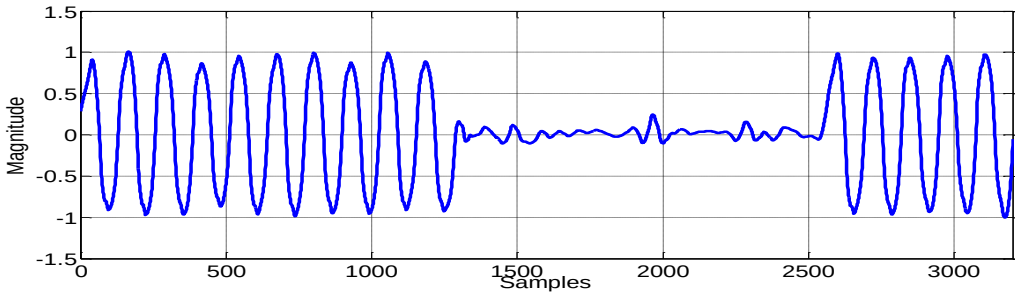


**Figure 3.3 (a) De-noised interruption disturbance**

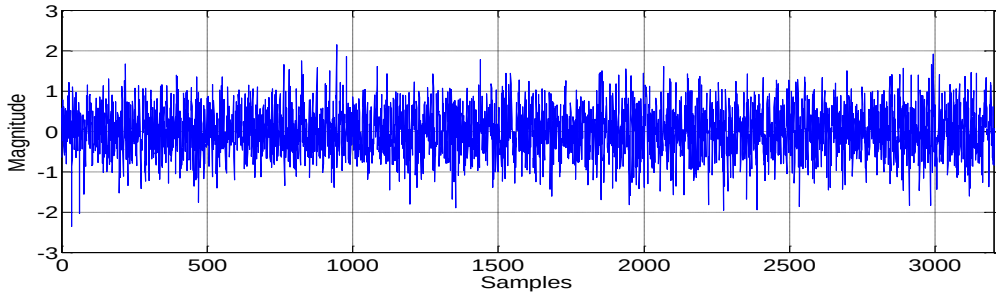


**Figure 3.3 (b) Amount of noise cleared**

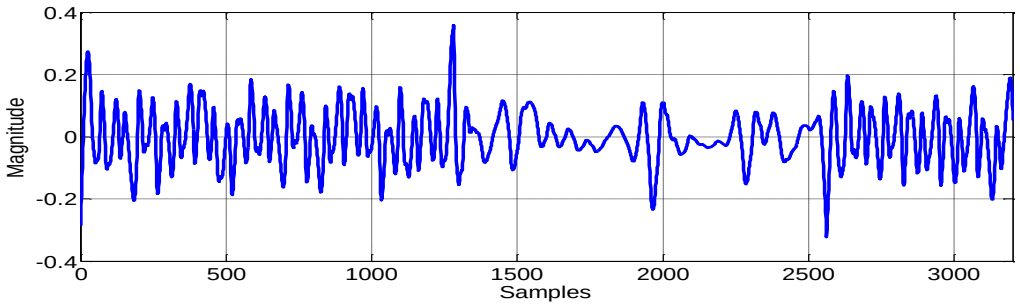


**Figure 3.3 (c) Residue after de-noising**

Figure 3.3 (a) is the de-noised Sag disturbance obtained after the implementation of the de-noising technique mentioned above in section 3.2.2. Figure 3.3(b) shows the amount of noise cleared which is obtained by subtracting the de-noised signal shown in Figure 3.3(a) from the noisy disturbance shown in Figure 2.18 in previous chapter.Figure 3.3(c) shows the residue after de-noising which is obtained by subtracting the de-noised signal obtained in Figure 3.3(a) from the Swell disturbance shown in Figure 2.6(b) in previous chapter.

## 3.4 Performance indices

The Effectiveness of a denoising technique can be measured or quantified based on certain performance parameters such as MSE(mean square error) and SNR(signal to noise ratio).If the MSE is lower and SNR is higher after the de-noising it represents a good de-noising technique.

*Mean Square Error:* Effectiveness of a de-noising scheme is also evaluated by mean square error (*MSE)* defined as

$$MSE = \frac{1}{N}\sum_{i=1}^{N}(V(i)-D(i))^2 \tag{3.5}$$

Where *D(i)* =De-noised Signal obtained

*V(i)* =Reference Power Quality Signal without Noise

N=Length of the Signal

*Signal to Noise Ratio:* The signal to noise ratio (*SNR)* is defined as

$$SNR(dB) = 10\log_{10}\frac{\sum_{i=1}^{N}V^2(i)}{\sum_{i=1}^{N}(V(i)-D(i))^2} \tag{3.6}$$

An effective de-noising method requires low mean square error (MSE) and high SNR.Table3.1 shows the performance indices for Sag, Swell and Interruption disturbance.

**Table3.1 Performance Indices**

| Type of Disturbance | MSE | SNR after De-noising(dB) |
|---|---|---|
| Sag | 0.0033 | 20.3171 |
| Swell | 0.0292 | 14.0962 |
| Interruption | 0.0097 | 14.9200 |

## 3.5 Summary

The results obtained in this chapter shows that the wavelet transform can be used effectively to de-noise different power quality disturbances. In this chapter a thresholding based de-noising technique is discussed which is quite efficient in de-noise different PQ events. The efficiency of the de-noising is evident from the performance parameters. A system can never be completely noise free as it is an ideal case. But with the help of the technique discussed above adequate amount of noise can be cleared which ensures very less percentage of noise in feature vector and hence improves the classification accuracy.

## 4.1 Introduction

The feature extraction is an important task in designing a monitoring system which will indicate the type of PQ disturbance occurring in the power system. A database is needed to be prepared based on some distinct parameters which will help in distinguishing different PQ disturbances with least amount of ambiguity. In this work after de-noising of PQ events, total harmonic distortion (THD) and Energy of the signal are used as the two distinctive parameters for feature extraction and preparing of the database. These databases are used as input to the fuzzy expert system for the classification purpose and also these databases are required to train the neural network so that a power quality disturbance (PQD) detection system can be modelled.

## 4.2 Feature vector

### 4.2.1 Total harmonic distortion

The distortion harmonics that included in each frequency ranges can be detected by using the approximation and the detailed coefficients which measure from sub band harmonics in terms of RMS value as (4.1)

$$RMS = \sqrt{\frac{1}{N_j}\sum_{n}\left[cD_j(n)\right]^2} \tag{4.1}$$

Where $N_j$ is the no of detail coefficients at scale $j$ while THD is calculated by considering each sub-band contribution [11-12] as shown in equation (4.2).The sampling frequency selected is 6.4 kHz or $128f_1$. In this paper, the fundamental frequency is 50 hertz and used six level of WT thus the output should receive the sub-band as follows:

• cD1: $32f_1 \sim 64f_1$;

• cD2: $16\ f_1 \sim 32\ f_1$;

• cD3: $8\ f_1 \sim 16\ f_1$;

• cD4: $4\ f_1 \sim 8\ f_1$;

• cD5: $2\ f_1 \sim 4\ f_1$;

• cD6: $1\ f_1 \sim 2\ f_1$;

• cA6: $0\ f_1 \sim 1\ f_1$;

$$THD = \frac{\sqrt{\frac{1}{N_j}\sum_n \left[cD_j(n)\right]^2}}{\sqrt{\frac{1}{N_6}\sum_n \left[cA_6(n)\right]^2}} \tag{4.2}$$

Where $N_j$ is the no of detail coefficients at scale *j*.

### 4.2.2 Energy of the signal

The energy of the signal is calculated using parseval's theorem [10] which states that if *S(t)* is the voltage across the resistor or current through the resistor then the energy dissipated is

$$E = \int_{-\infty}^{\infty} \left|S(t)\right|^2 dt \tag{4.3}$$

In wavelet domain the signal is decomposed into the approximate and detailed coefficients and therefore energy dissipated by the signal in terms of approximate and detail coefficients given by equation. (4.4)

$$E = \sum_k \left|C_j(k)\right|^2 + \sum_{j=1}^{I}\sum_k \left|D_j(k)\right|^2 \tag{4.4}$$

Where $C_j(k)$ is approximate coefficient at *j*th level and $D_j(k)$ is detail coefficient at *j*th level.

## 4.3 Database of different PQ disturbances

A database of THD and Energy of different PQ disturbances as discussed in section 4.2 based on equation (4.2) and equation (4.4) is prepared.Diferent PQ disturbances with different magnitude of fault is generated and considered for feature extraction. The change in the time of occurrence of the short duration disturbance in the signals do not change the values of feature vector much the change can be found only when the duration of short duration disturbance changes [19].Here the duration of disturbance is kept at 0.2 second though the occurrence of the disturbance is varied.

### 4.3.1 Voltage Sag

The voltage sag is a decrease of 10-90% of the rated system voltage for duration of 0.5 cycles to 1 min.Hence a data base of Energy and THD is prepared for 10-90% drop in system voltage. Table 4.1 shows the feature vector for voltage sag.

**Table.4.1 Feature vector for voltage sag**

| MAGNITUDE OF DISTURBANCE(%) | THD | ENERGY(volt$^2$ –sec) |
|---|---|---|
| 10 | 0.7411 | $1.4906*10^3$ |
| 20 | 0.7418 | $1.3818*10^3$ |
| 30 | 0.7426 | $1.2858*10^3$ |
| 40 | 0.7433 | $1.2026*10^3$ |
| 50 | 0.7441 | $1.1322*10^3$ |
| 60 | 0.7448 | $1.0746*10^3$ |
| 70 | 0.7454 | $1.0928*10^3$ |
| 80 | 0.7460 | 997.7708 |
| 90 | 0.7464 | 978.5708 |

From the Table 4.1 it is observed that as the magnitude of fault increases the value of THD also increases but the Energy goes on decreasing with the increase in the magnitude of fault.

### 4.3.2 Voltage swell

In the case of voltage swell, there is a rise of 10-90% in the voltage magnitude for 0.5 cycles to 1 min. Hence a data base of Energy and THD is prepared for 10-90% rise in system voltage or 110-190% of magnitude of fault. Table 4.2 shows the feature vector for voltage swell.

**Table.4.2 Feature vector for voltage swell**

| MAGNITUDE OF DISTURBANCE(%) | THD | ENERGY(volt$^2$ –sec) |
|---|---|---|
| 110 | 0.7399 | $1.7466*10^3$ |
| 120 | 0.7394 | $1.8938*10^3$ |
| 130 | 0.7390 | $2.0538*10^3$ |
| 140 | 0.7386 | $2.2266*10^3$ |
| 150 | 0.7382 | $2.4122*10^3$ |
| 160 | 0.7379 | $2.6106*10^3$ |
| 170 | 0.7377 | $2.8218*10^3$ |
| 180 | 0.7375 | $3.0458*10^3$ |
| 190 | 0.7373 | $3.2826*10^3$ |

From Table 4.2 it is observed that the THD goes on decreasing with the increase in the magnitude of the disturbance but the Energy goes on increasing with the magnitude of disturbance, opposite to the characteristic of Voltage sag.

### 4.3.3 Voltage interruption

The voltage interruption may be seen as a loss of voltage in a power system. Such disturbance describes a drop of 90-100% of the rated system voltage for duration of 0.5 cycles to 1 min.Hence a database of 1-9% of magnitude of fault is prepared which is shown in Table 4.3.

**Table.4.3 Feature vector for voltage interruption**

| MAGNITUDE OF DISTURBANCE(%) | THD | ENERGY(volt$^2$ –sec) |
|---|---|---|
| 1 | 0.7467 | 972.2988 |
| 2 | 0.7466 | 972.6828 |
| 3 | 0.7463 | 973.3228 |
| 4 | 0.7460 | 974.2188 |
| 5 | 0.7455 | 975.3708 |
| 6 | 0.7449 | 976.7788 |
| 7 | 0.7442 | 978.4428 |
| 8 | 0.7443 | 980.3628 |
| 9 | 0.7424 | 982.5388 |

From Table 4.3 it is observed that while the THD goes on decreasing the Energy goes on increasing with the increase in the fault magnitude but the variation in Energy and THD level is very small.

### 4.3.4 Voltage Surge

In Voltage surge the amplitude of the voltage is suddenly increased due to the disconnection of a heavy load for one quarter of a cycle. Here only 160-240% rise in the system voltage is considered under voltage surge. Table 4.4 shows the database of voltage surge which is prepared for 160-240% of magnitude of fault. From table 4.4 it is observed that with the increase in the magnitude of the fault the THD and the Energy also increases though the variation in both the THD and the Energy is very less with increase in the fault magnitude.

**Table 4.4 Feature vector for voltage surge**

| MAGNITUDE OF DISTURBANCE(%) | THD | ENERGY($volt^2$ –sec) |
|---|---|---|
| 160 | 0.8011 | $1.6155*10^3$ |
| 170 | 0.8023 | $1.6158*10^3$ |
| 180 | 0.8036 | $1.6161*10^3$ |
| 190 | 0.8048 | $1.6165*10^3$ |
| 200 | 0.8061 | $1.6169*10^3$ |
| 210 | 0.8074 | $1.6173*10^3$ |
| 220 | 0.8087 | $1.6177*10^3$ |
| 230 | 0.8100 | $1.6182*10^3$ |
| 240 | 0.8113 | $1.6187*10^3$ |

The complex disturbances like Voltage sag with harmonics, voltage swell with harmonics and voltage interruption with harmonics are also considered in this work. The magnitude of the fault remains the same as in the case of normal voltage sag, swell and interruption. Here only $3^{rd}$, $5^{th}$ and $7^{th}$ order of harmonics is considered in each case as these three are the most dominant and frequently occurring harmonics in the power system.

### 4.3.5 Voltage sag with harmonics

Table 4.5, 4.6 and 4.7 shows the feature vector for voltage sag with harmonics of $3^{rd}$ ,$5^{th}$ and $7^{th}$ order harmonics respectively.

**Table 4.5 Feature vector for voltage sag with $3^{rd}$ order harmonics**

| MAGNITUDE OF DISTURBANCE(%) | THD | ENERGY($volt^2$ –sec) |
|---|---|---|
| 10 | 1.5089 | $3.1721*10^3$ |
| 20 | 1.5405 | $3.0633*10^3$ |
| 30 | 1.5717 | $2.9673*10^3$ |
| 40 | 1.6019 | $2.8841*10^3$ |
| 50 | 1.6305 | $2.8173*10^3$ |
| 60 | 1.6567 | $2.7561*10^3$ |
| 70 | 1.6798 | $2.7113*10^3$ |
| 80 | 1.6990 | $2.6793*10^3$ |
| 90 | 1.7137 | $2.6601*10^3$ |

**Table 4.6 Feature vector for voltage sag with $5^{th}$ order harmonics**

| MAGNITUDE OF DISTURBANCE(%) | THD | ENERGY($volt^2$ –sec) |
|---|---|---|
| 10 | 1.4242 | $3.2069*10^3$ |
| 20 | 1.4520 | $3.0981*10^3$ |
| 30 | 1.4795 | $3.0021*10^3$ |
| 40 | 1.5059 | $2.9189*10^3$ |
| 50 | 1.5309 | $2.8485*10^3$ |
| 60 | 1.5537 | $2.7909*10^3$ |
| 70 | 1.5738 | $2.7461*10^3$ |
| 80 | 1.5904 | $2.7141*10^3$ |
| 90 | 1.6031 | $2.6949*10^3$ |

**Table 4.7 Feature vector for voltage sag with 7th order harmonics**

| MAGNITUDE OF DISTURBANCE(%) | THD | ENERGY(volt$^2$ –sec) |
|---|---|---|
| 10 | 1.4394 | $3.2600*10^3$ |
| 20 | 1.4609 | $3.1512*10^3$ |
| 30 | 1.4815 | $3.0552*10^3$ |
| 40 | 1.5007 | $2.9720*10^3$ |
| 50 | 1.5180 | $2.9016*10^3$ |
| 60 | 1.5327 | $2.8440*10^3$ |
| 70 | 1.5445 | $2.7992*10^3$ |
| 80 | 1.5528 | $2.7672*10^3$ |
| 90 | 1.5572 | $2.7480*10^3$ |

From the Table 4.5, 4.6 and 4.7 it is observed that THD value is quite large than the case of normal voltage sag without the harmonics. This is because of the presence of harmonics which results in increase of both THD and Energy of the disturbance considerably.

### 4.3.6 Voltage swell with harmonics

Table 4.8, 4.9 and 4.10 shows the feature vector for voltage swell with harmonics of 3rd ,5th and 7th order harmonics respectively.

**Table 4.8 Voltage swell with 3rd order harmonics**

| MAGNITUDE OF DISTURBANCE(%) | THD | ENERGY(volt$^2$ –sec) |
|---|---|---|
| 110 | 1.4461 | $3.4281*10^3$ |
| 120 | 1.4156 | $3.5753*10^3$ |
| 130 | 1.3859 | $3.7353*10^3$ |
| 140 | 1.3573 | $3.9081*10^3$ |
| 150 | 1.3299 | $4.0937*10^3$ |
| 160 | 1.3036 | $4.2921*10^3$ |
| 170 | 1.2785 | $4.5033*10^3$ |
| 180 | 1.2546 | $4.7273*10^3$ |
| 190 | 1.2319 | $4.9641*10^3$ |

**Table 4.9 Voltage swell with 5th order harmonics**

| MAGNITUDE OF DISTURBANCE(%) | THD | ENERGY(volt$^2$ –sec) |
|---|---|---|
| 110 | 1.3688 | $3.4629*10^3$ |
| 120 | 1.3419 | $3.6101*10^3$ |
| 130 | 1.3159 | $3.7701*10^3$ |
| 140 | 1.2907 | $3.9429*10^3$ |
| 150 | 1.2666 | $4.1285*10^3$ |
| 160 | 1.2436 | $4.3269*10^3$ |
| 170 | 1.2216 | $4.5381*10^3$ |
| 180 | 1.2008 | $4.7621*10^3$ |
| 190 | 1.1811 | $4.9989*10^3$ |

**Table 4.10 Voltage swell with 7th order harmonics**

| MAGNITUDE OF DISTURBANCE(%) | THD | ENERGY(volt$^2$ –sec) |
|---|---|---|
| 110 | 1.3953 | $3.5160*10^3$ |
| 120 | 1.3734 | $3.6632*10^3$ |
| 130 | 1.3518 | $3.8232*10^3$ |
| 140 | 1.3307 | $3.9960*10^3$ |
| 150 | 1.3103 | $4.1816*10^3$ |
| 160 | 1.2906 | $4.3800*10^3$ |
| 170 | 1.2717 | $4.5912*10^3$ |
| 180 | 1.2536 | $4.8152*10^3$ |
| 190 | 1.2363 | $5.0520*10^3$ |

Table 4.8, 4.9 and 4.10 reveals that the value of THD and Energy is quite higher than the value which is obtained in case of voltage swell without the harmonics due to the presence of harmonics only. It is also observed that value of Energy in case of voltage swell with 7th order harmonics is higher than 5th and 3rd order harmonics.

### 4.3.7 Interruption with harmonics

Table 4.11, 4.12 and 4.13 shows the feature vector for voltage interruption with harmonics of $3^{rd}$ ,$5^{th}$ and $7^{th}$ order harmonics respectively.

**Table 4.11 Voltage interruption with $3^{rd}$ order harmonics**

| MAGNITUDE OF DISTURBANCE(%) | THD | ENERGY($volt^2$ –sec) |
|---|---|---|
| 1 | 1.7233 | $2.6538*10^3$ |
| 2 | 1.7230 | $2.6542*10^3$ |
| 3 | 1.7224 | $2.6548*10^3$ |
| 4 | 1.7216 | $2.6557*10^3$ |
| 5 | 1.7205 | $2.6569*10^3$ |
| 6 | 1.7192 | $2.6583*10^3$ |
| 7 | 1.7177 | $2.6600*10^3$ |
| 8 | 1.7160 | $2.6619*10^3$ |
| 9 | 1.7140 | $2.6641*10^3$ |

**Table 4.12 Voltage interruption with $5^{th}$ order harmonics**

| MAGNITUDE OF DISTURBANCE(%) | THD | ENERGY($volt^2$ –sec) |
|---|---|---|
| 1 | 1.6113 | $2.6886*10^3$ |
| 2 | 1.6110 | $2.6890*10^3$ |
| 3 | 1.6104 | $2.6897*10^3$ |
| 4 | 1.6096 | $2.6906*10^3$ |
| 5 | 1.6085 | $2.6917*10^3$ |
| 6 | 1.6073 | $2.6931*10^3$ |
| 7 | 1.6058 | $2.6948*10^3$ |
| 8 | 1.6041 | $2.6967*10^3$ |
| 9 | 1.6022 | $2.6989*10^3$ |

**Table 4.13 Voltage interruption with 7th order harmonics**

| MAGNITUDE OF DISTURBANCE(%) | THD | ENERGY(volt$^2$ –sec) |
|---|---|---|
| 1 | 1.5575 | $2.7417*10^3$ |
| 2 | 1.5571 | $2.7421*10^3$ |
| 3 | 1.5565 | $2.7427*10^3$ |
| 4 | 1.5557 | $2.7436*10^3$ |
| 5 | 1.5546 | $2.7448*10^3$ |
| 6 | 1.5533 | $2.7462*10^3$ |
| 7 | 1.5518 | $2.7479*10^3$ |
| 8 | 1.5500 | $2.7498*10^3$ |
| 9 | 1.5481 | $2.7520*10^3$ |

From Table 4.11, 4.12 and 4.13 it can be concluded that value of THD in case of 3rd harmonics is more as compared to 5th and 7th order harmonics of voltage interruption. Similarly value of Energy in case of 7th order harmonics is higher as compared to other two harmonics. Also the value of THD is the highest in case of Voltage interruption with 3rd harmonics than any other PQ disturbances.

## 4.4 Summary

In this part of the work different PQ disturbances with different fault magnitude are generated and the feature vector containing Energy and THD are extracted based on the equation (4.2) and equation (4.4) as discussed in section 4.2 and a database is prepared. It is observed that the value of THD and Energy is increased considerably if the PQ disturbance contains harmonics. It is also observed that value of Energy in case of voltage swell with 7th order harmonics is the highest among all other PQ disturbances. Similarly the value of the Energy is lowest in case of voltage interruption. It is also observed that THD in case of voltage interruption with 7th order harmonics is the highest among all. These databases will be used in training the neural network for modelling a PQD detection system. Also these databases are going to be used in designing a fuzzy expert system for the classification purpose.

## 5.1 Introduction

The work on Neural Networks (NN) was inspired from the way the human brain operates. Our brain is a highly non-linear, complex and parallel computer-like device. It has the ability to organize its structural constituents known as neurons, so as to carry out certain computations (e.g. perception, pattern recognition and motor control) much faster than the fastest digital computer in existence today. This ability of our brain has been utilized into processing units to further excel in the field of artificial intelligence. The theory of modern neural networks began by the pioneering works done by Pitts (a Mathematician) and McCulloh (a psychiatrist) in 1943. This Chapter details the attempt at modeling of the power quality disturbance (PQD) detection system using Multilayer Feedforward Neural Network (MFNN).

## 5.2 Multilayer Feedforward Neural Network

### 5.2.1 MFNN Structure

Artificial Neural Networks (ANNs) have become the subject of widespread interest, largely because of their wide range of applicability and the ease with which they handle complex and non-linear problems. They are massively parallel-interconnected networks of simple elements intended to interact with the real world in the same way as the biological nervous system. They offer an unusual scheme based programming standpoint and exhibit higher computing speeds compared to other conventional methods. ANNs are characterized by their topology, that is, the number of interconnections, the node characteristics that are classified by the type of nonlinear elements used and the kind of learning rules employed. The ANN is composed of an organized topology of Processing Elements (PEs) called neurons. In Multilayer Feedforward Neural Network (MFNN) the PEs are arranged in layers and only PEs in adjacent layers are connected. The MFNN structure used in this thesis consists of three layers, namely, the input layer, the hidden layer and the output layer as shown in Figure 5.1.

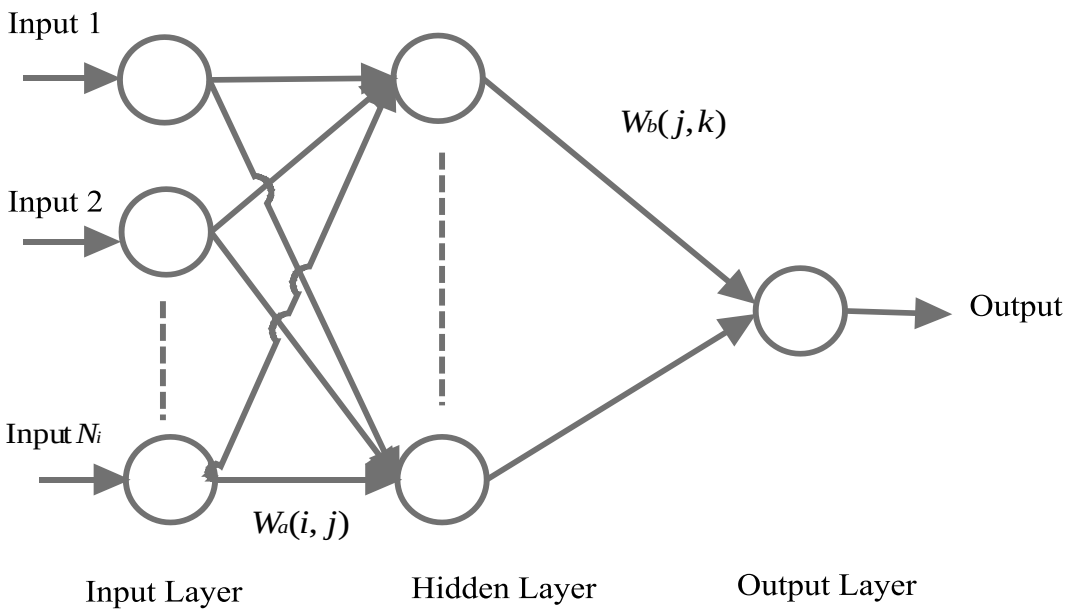


**Figure 5.1 Multilayer Feedforward Neural Network**

The input layer consists of $N_i$ neurons corresponding to the $N_i$ inputs. The number of output neurons is decided by the number of predicted parameters. The Back Propagation Algorithm (BPA) is used to train the network. The sigmoidal function represented by equation (5.1) is used as the activation function for all the neurons except for those in the input layer.

$$S(x) = 1 / (1+e^{-x}) \quad (5.1)$$

### 5.2.2 Back Propagation Algorithm

Backpropagation is a well-known method for teaching artificial neural networks so as how to do a given task. It was first explained by Arthur E. Bryson and Yu-Chi Ho in 1969, but it was not until 1974, and later, through the work of Paul Werbos, David E. Rumelhart, Geoffrey E. Hinton and Ronald J. Williams, that it became popular.

It is a method of supervised learning that can be visualized as a generalization of the delta rule. It demands a teacher that knows, or can find out, the desired output for any input in training set. It is extremely effective for feedforward networks. The term is an abbreviation for "backward propagation of errors". Back propagation demands that the activation function which is used by the artificial neurons has to be differentiable. For understanding, the back

propagation learning algorithm can be divided into two phases.phase: 1.propagation and phase: 2.weight update.

Phase 1: Propagation

Each propagation module comprises the following steps:

1. Forward propagation of a training data pattern's input through neural network in order to produce the propagation's output activations.

2. Backward propagation of the propagation's output activations through the neural

network by using training pattern's target to generate the deltas of all output and hidden neurons.

Phase 2: Weight update

For every weight-synapse:

1. The output delta and input activation is to be multiplied to find gradient of the weight.

2. Bring the weight in the opposite direction of the gradient by subtracting a ratio of it from the weight.

This ratio has impact on the speed and quality of learning; it is therefore called the learning rate. The sign of the gradient of a weight signifies that where error is increasing, because of this the weight has to be updated in the opposite direction. Perform repetition of the phases 1 and 2 until the performance of the network is satisfactory.

### 5.2.3 Choice of Hidden Neurons

The choice of optimal number of hidden neurons, $N_h$ is the most interesting and challenging aspect in designing the MFNN. There are various schools on thought in deciding the value of $N_h$. Simon Haykin has specified that $N_h$ should lie between 2 and $\infty$. Hecht-Nielsen uses ANN interpretation of Kolmogorov's theorem to arrive at the upper bound on the $N_h$ for a single hidden layer network as $2(N_i+1)$, where $N_i$ is the number of input neurons. However, this value should be decided very judiciously depending on the requirement of a problem. A large value of $N_h$ may reduce the training error associated with the MFNN, but at the cost of increasing the computational complexity and time. For example, if one gets a

tolerably low value of training error with certain value of $N_h$, there is no point in further increasing the value of $N_h$ to enhance the performance of the MFNN.

### 5.2.4 Normalization of Input-Output data

The input and the output data are normalized before being processed in the network. In this scheme of normalization, the maximum values of the input and output vector components are determined as follows:

$$n_{i,\max} = \max(n_i(p)) \quad p = 1,\ldots\ldots, N_p, \quad i = 1,\ldots\ldots, N_i \tag{5.2}$$

Where $N_p$ is the number of patterns in the training set

$$o_{k,\max} = \max(o_k(p)) \quad p = 1,\ldots\ldots N_p, \quad i = 1,\ldots\ldots N_k \tag{5.3}$$

Where $N_k$ is the number of neurons in the output layer, that is, the number of predicted parameters.

Normalized by these maximum values, the input and output variables are obtained as follows:

$$n_{i,nor}(p) = \frac{n_i(p)}{n_{i,\max}} \qquad p = 1,\ldots\ldots, N_p, \quad i = 1,\ldots\ldots, N_i \tag{5.4}$$

and

$$o_{k,nor}(p) = \frac{o_k(p)}{o_{k,\max}} \qquad p = 1,\ldots\ldots N_p, \quad i = 1,\ldots\ldots N_k \tag{5.5}$$

After normalization, the input and output variables lie in the range of 0 to 1.

### 5.2.5 Choice of ANN parameters

The learning rate, $\eta_1$ and the momentum factor, $\alpha_1$ have a very significant effect on the learning speed of the BPA. The BPA provides an approximation to the trajectory in the weight space computed by the method of steepest descent method. If the value of $\eta_1$ is considered very small, this results in slow rate of learning, while if the value of $\eta_1$ is too large in order to speed up the rate of learning, the MFNN may become unstable (oscillatory). A simple method of increasing the rate of learning without making the MFNN unstable is by adding the momentum factor $\alpha_1$. Preferably, the values of $\eta_1$ and $\alpha_1$ should lie between 0 and 1.

### 5.2.6 Weight Update Equations

The weights between the hidden layer and the output layer are updated based on the equation (5.6) as follows:

$$w_b(j,k,m+1) = w_b(j,k,m)+\eta_1*\delta_k(m) *S_b(j) + \alpha_1 [w_b(j, k, m) - w_b(j, k, m-1)] \quad (5.6)$$

Where m is the number of iterations, j varies from 1 to $N_h$ and k varies from 1 to $N_k$. $\delta_k(m)$ is the error for the $k^{th}$ output at the $m^{th}$ iteration. $S_b(j)$ is the output from the hidden layer.

Similarly, the weights between the hidden layer and the input layer are updated as follows:

$$w_a(i,j,m+1)=w_a(i,j,m)+\eta_1*\delta_j(m)*S_a(i) + \alpha_1 [(w_a(i, j, m) - w_a(i, j, m-1)] \quad (5.7)$$

Where i varies from 1 to $N_i$ as there are $N_i$ inputs to the network, $\delta_j(m)$ is the error for the $j^{th}$ output after the $m^{th}$ iteration and $S_a(i)$ is the output from the first layer. The $\delta_k(m)$ in equation (5.6) and $\delta_j(m)$ in equation ( 5.7) are related as

$$\delta_j(m)=\sum_{k=1}^{K} \delta_k(m)*w_b(j,k,m) \quad (5.8)$$

### 5.2.7 Evaluation Criterion

The Mean Square Error $E_{tr}$ for the training patterns after the $m^{th}$ iteration is defined as

$$E_{tr}(m)=(1/N_p)*[\sum_{p=1}^{Np} \{PD_{1p}–PD_{2p}(m)\}^2] \quad (5.9)$$

Where $PD_{1p}$ is the exact value of the percentage of disturbance in voltage. $PD_{2p}(m)$ is the estimated value of the percentage of disturbance in voltage after $m^{th}$ iteration. The training is stopped when the least value of $E_{tr}$ has been obtained and this value does not change much with the number of iterations.

The Mean Absolute Error Ets is a good performance measure for judging the accuracy of the MFNN System. The $E_{tr}$ tells how well the network has adopted to fit the training data only, even if the data are contaminated. On the other hand, the $E_{ts}$ indicates how well a trained network behaves on a new data set not included in the training set. The value of $E_{ts}$ is calculated based on the least value of $E_{tr}$. The $E_{ts}$ for the test data expressed in percentage is given by

$$E_{ts} = (1/N_S) * [\sum_{s=1}^{Ns} |(PD_{4s} - PD_{3s})|/PD_{3s}] * 100 \quad (5.10)$$

Where $PD_{3s}$ is the exact value of percentage of disturbance in voltage taken for testing purpose, $PD_{4s}$ is the estimated value of the percentage of disturbance in voltage after the test input data is passed through the trained network and $N_s$ is the number of test patterns.

## 5.3 Modeling of PQD Detection System Using MFNN

This section details the attempt at modeling a detection system for power quality disturbances using MFNN. This model predicts the percentage of disturbance in various power quality events as a function of Energy and THD of different power quality events. The network is provided with both input data and desired response and is trained in a supervised manner using the back propagation algorithm. The back propagation algorithm performs the input to output mapping by making weight connection adjustment following the discrepancy between the computed output value and the desired output response. The training phase is completed after a series of iterations. In each iteration, output is compared with the desired response and a match is obtained. Figure 5.2 is derived from Figure 1.1 which shows the different steps involved in modeling of PQD detection system. Figure5.3 shows the flowchart for the MFNN.

In order to predict the percentage of disturbance a software program has been developed in MATLAB 7.10 to solve equations (5.1) to (5.10).

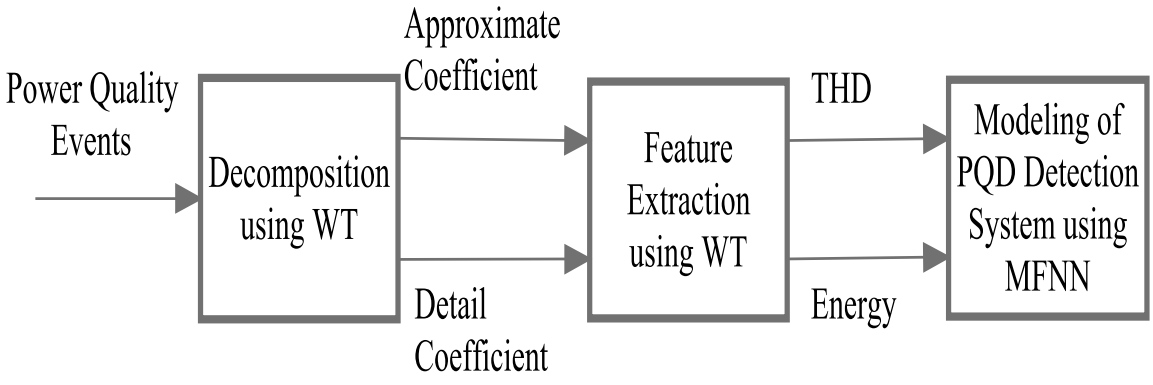


**Figure 5.2 Processes involved in Modeling of PQD Detection system**

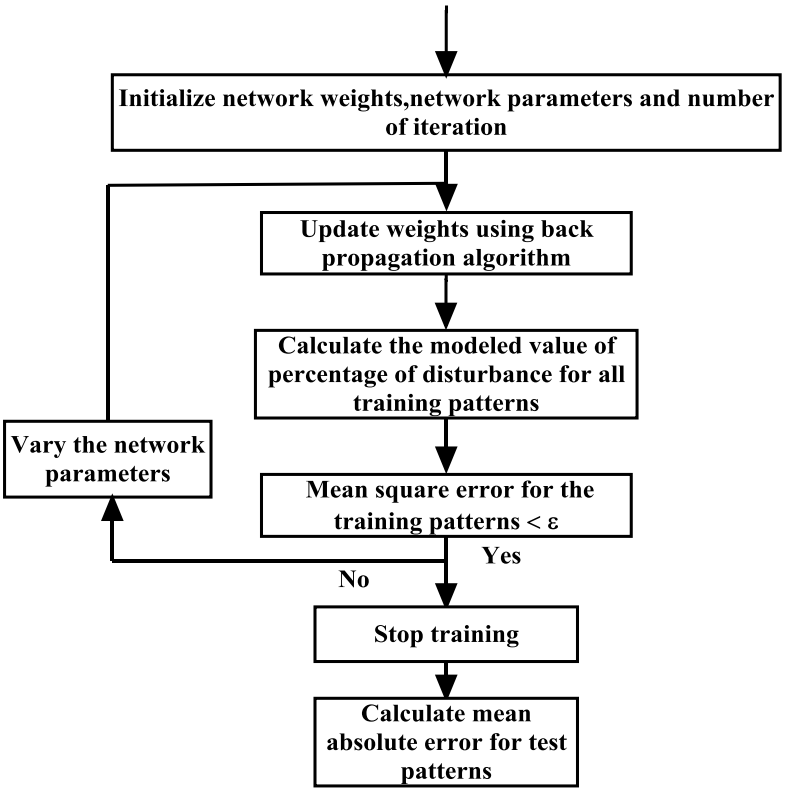


**Figure 5.3 Flow chart of MFNN**

In this model, the number of input parameters is two, that is, the energy and THD of different power quality disturbances. The energy of the PQ disturbances is **e** and THD is **d** and percentage of disturbance is to be predicted. Since, the input parameters are two, the value of $N_i$ is two for this model. In addition, since the output parameter is only one, the value of $N_k$ is one.

The total number of PQ disturbances considered for the purpose of modeling is five such as voltage sag, voltage swell, interruption, sag with harmonics and swell with harmonics. There are 25 sets of PQ events are generated for each of the five different PQ disturbances using MATLAB 7.10 and input-output data sets were found out for each case using the feature extraction process as discussed in previous section. Hence a total of 125 input-output data sets are generated as given in Table 5.1 and out of which 110 data sets are used for training the MFNN model and finding the mean square error. The rest 15 sets of input-output data are used for testing purpose which is also used for calculating mean absolute error.

**Table 5.1 Input-Output data sets**

| Serial number | Type of disturbance | Energy | THD | Percentage of disturbance estimated |
|---|---|---|---|---|
| 1 | Sag | 1490.6 | 0.7411 | 10 |
| 2 | | 1467.8 | 0.7413 | 12 |
| 3 | | 1434.6 | 0.7415 | 15 |
| 4 | | 1402.5 | 0.7417 | 18 |
| 5 | | 1381.8 | 0.7418 | 20 |
| 6 | | 1361.5 | 0.7420 | 22 |
| 7 | | 1332.2 | 0.7422 | 25 |
| 8 | | 1285.8 | 0.7426 | 30 |
| 9 | | 1268.1 | 0.7427 | 32 |
| 10 | | 1251 | 0.7429 | 34 |
| 11 | | 1234.3 | 0.7430 | 36 |
| 12 | | 1202.6 | 0.7433 | 40 |
| 13 | | 1172.9 | 0.7436 | 44 |
| 14 | | 1158.8 | 0.7438 | 46 |
| 15 | | 1138.6 | 0.7440 | 49 |
| 16 | | 1119.6 | 0.7442 | 52 |
| 17 | | 1101.8 | 0.7445 | 55 |
| 18 | | 1074.6 | 0.7448 | 60 |
| 19 | | 1064.6 | 0.7449 | 62 |
| 20 | | 1050.6 | 0.7451 | 65 |
| 21 | | 1037.7 | 0.7453 | 68 |
| 22 | | 1029.8 | 0.7454 | 70 |
| 23 | | 1012.2 | 0.7457 | 75 |
| 24 | | 1003.1 | 0.7459 | 78 |
| 25 | | 997.7 | 0.7460 | 80 |

Continued

| Serial number | Type of disturbance | Energy | THD | Percentage of disturbance estimated |
|---|---|---|---|---|
| 26 | Swell | 1746.6 | 0.7399 | 110 |
| 27 | | 1775 | 0.7398 | 112 |
| 28 | | 1818.6 | 0.7397 | 115 |
| 29 | | 1863.3 | 0.7395 | 118 |
| 30 | | 1893.8 | 0.7394 | 120 |
| 31 | | 1924.7 | 0.7393 | 122 |
| 32 | | 1972.2 | 0.7392 | 125 |
| 33 | | 2053.8 | 0.7390 | 130 |
| 34 | | 2087.3 | 0.7389 | 132 |
| 35 | | 2121.4 | 0.7388 | 134 |
| 36 | | 2191 | 0.7386 | 138 |
| 37 | | 2226.6 | 0.7386 | 140 |
| 38 | | 2317.8 | 0.7384 | 145 |
| 39 | | 2374 | 0.7383 | 148 |
| 40 | | 2412.2 | 0.7382 | 150 |
| 41 | | 2490 | 0.7381 | 154 |
| 42 | | 2569.9 | 0.7380 | 158 |
| 43 | | 2610.6 | 0.7379 | 162 |
| 44 | | 2714.6 | 0.7378 | 165 |
| 45 | | 2821.8 | 0.7377 | 170 |
| 46 | | 2865.5 | 0.7376 | 172 |
| 47 | | 2909.8 | 0.7376 | 174 |
| 48 | | 2999.9 | 0.7375 | 178 |
| 49 | | 3045.8 | 0.7375 | 180 |
| 50 | | 3162.6 | 0.7374 | 185 |

Continued

| Serial number | Type of disturbance | Energy | THD | Percentage of disturbance estimated |
|---|---|---|---|---|
| 51 | Interruption | 972.2988 | 0.7467 | 1 |
| 52 | | 972.3551 | 0.7467 | 1.2 |
| 53 | | 972.4217 | 0.7466 | 1.4 |
| 54 | | 972.4985 | 0.7466 | 1.6 |
| 55 | | 972.5855 | 0.7466 | 1.8 |
| 56 | | 972.6828 | 0.7466 | 2 |
| 57 | | 972.7903 | 0.7465 | 2.2 |
| 58 | | 972.9081 | 0.7465 | 2.4 |
| 59 | | 972.9708 | 0.7465 | 2.5 |
| 60 | | 973.1039 | 0.7464 | 2.7 |
| 61 | | 973.2473 | 0.7464 | 2.9 |
| 62 | | 973.4815 | 0.7463 | 3.2 |
| 63 | | 973.7388 | 0.7462 | 3.5 |
| 64 | | 974.2188 | 0.7460 | 4 |
| 65 | | 974.4827 | 0.7459 | 4.2 |
| 66 | | 974.6489 | 0.7458 | 4.4 |
| 67 | | 974.8793 | 0.7457 | 4.6 |
| 68 | | 975.1199 | 0.7456 | 4.8 |
| 69 | | 975.3708 | 0.7455 | 5 |
| 70 | | 975.9033 | 0.7453 | 5.4 |
| 71 | | 976.1849 | 0.7452 | 5.6 |
| 72 | | 976.4767 | 0.7450 | 5.8 |
| 73 | | 977.0911 | 0.7448 | 6.2 |
| 74 | | 977.5788 | 0.7446 | 6.5 |
| 75 | | 978.4428 | 0.7442 | 7 |

Continued

| Serial number | Type of disturbance | Energy | THD | Percentage of disturbance estimated |
|---|---|---|---|---|
| 76 | Sag with harmonics | 3172.1 | 1.5089 | 10 |
| 77 | | 3149.3 | 1.5152 | 12 |
| 78 | | 3116.1 | 1.5247 | 15 |
| 79 | | 3084 | 1.5342 | 18 |
| 80 | | 3063.3 | 1.5405 | 20 |
| 81 | | 3023.4 | 1.5531 | 24 |
| 82 | | 2985.5 | 1.5655 | 28 |
| 83 | | 2967.3 | 1.5717 | 30 |
| 84 | | 2949.6 | 1.5779 | 32 |
| 85 | | 2924.1 | 1.5870 | 35 |
| 86 | | 2899.7 | 1.5960 | 38 |
| 87 | | 2884.1 | 1.6019 | 40 |
| 88 | | 2869 | 1.6078 | 42 |
| 89 | | 2840.3 | 1.6193 | 46 |
| 90 | | 2826.7 | 1.6249 | 48 |
| 91 | | 2813.7 | 1.6305 | 50 |
| 92 | | 2801.1 | 1.6359 | 52 |
| 93 | | 2777.6 | 1.6445 | 56 |
| 94 | | 2756.1 | 1.6567 | 60 |
| 95 | | 2746.1 | 1.6616 | 62 |
| 95 | | 2732.1 | 1.6687 | 65 |
| 96 | | 2719.2 | 1.6754 | 68 |
| 97 | | 2711.3 | 1.6798 | 70 |
| 98 | | 2697 | 1.6880 | 74 |
| 99 | | 2679.3 | 1.6990 | 80 |
| 100 | | 2678 | 1.7140 | 84 |

Continued

| Serial number | Type of disturbance | Energy | THD | Percentage of disturbance estimated |
|---|---|---|---|---|
| 101 | Swell with harmonics | 3428.1 | 1.4461 | 110 |
| 102 | | 3456.5 | 1.4399 | 112 |
| 103 | | 3485.4 | 1.4338 | 114 |
| 104 | | 3544.8 | 1.4216 | 118 |
| 105 | | 3575.3 | 1.4156 | 120 |
| 106 | | 3637.8 | 1.4036 | 124 |
| 107 | | 3702.3 | 1.3918 | 128 |
| 108 | | 3735.3 | 1.3859 | 130 |
| 109 | | 3768.8 | 1.3801 | 132 |
| 110 | | 3802.9 | 1.3744 | 134 |
| 111 | | 3872.5 | 1.3630 | 138 |
| 112 | | 3908.1 | 1.3573 | 140 |
| 113 | | 3980.8 | 1.3462 | 144 |
| 114 | | 4055.5 | 1.3353 | 148 |
| 115 | | 4093.7 | 1.3299 | 150 |
| 116 | | 4171.5 | 1.3192 | 154 |
| 117 | | 4251.4 | 1.3088 | 158 |
| 118 | | 4292.1 | 1.3036 | 160 |
| 119 | | 4396.1 | 1.2909 | 165 |
| 120 | | 4460 | 1.2834 | 168 |
| 121 | | 4503.3 | 1.2785 | 170 |
| 122 | | 4591.4 | 1.2688 | 174 |
| 123 | | 4681.5 | 1.2593 | 178 |
| 124 | | 4727.3 | 1.2546 | 180 |
| 125 | | 4773.6 | 1.2500 | 182 |

## 5.4 Results and Discussions

In this study, the optimum values of network parameters are obtained based on Mean Square Error $E_{tr}$ for the training patterns. The network is trained in a sequential mode. In applying the BPA for the proposed prediction work the following key issues are addressed

1. Network parameters
2. Number of hidden neurons
3. Number of iterations

For BPA with fixed values of learning rate η and momentum factor α, the optimum values are obtained by simulation with different values of η and α. So, to start with a value of η =0.3and α = 0.1 are chosen and then varied to get an optimum value. It may be noted that the range of values of η and α should be between 0 and 1. Finally, a best combination is seem to yield with a value of η= 0.99 and α=0.85. For the above combination and with six hidden neurons the value $E_{tr}$ is decreasing to a lowest value of $1.3202*10^{-9}$. The network structure is thus as shown in Figure 5.4. The variation of $E_{tr}$ of the training data with the number of iterations with η= 0.99, α=0.85, $N_h$=6.0 is shown in Figure 5.5.Tables 5.2-5.5 shows the variation of $E_{tr}$ as a function of η, α and $N_h$ respectively.

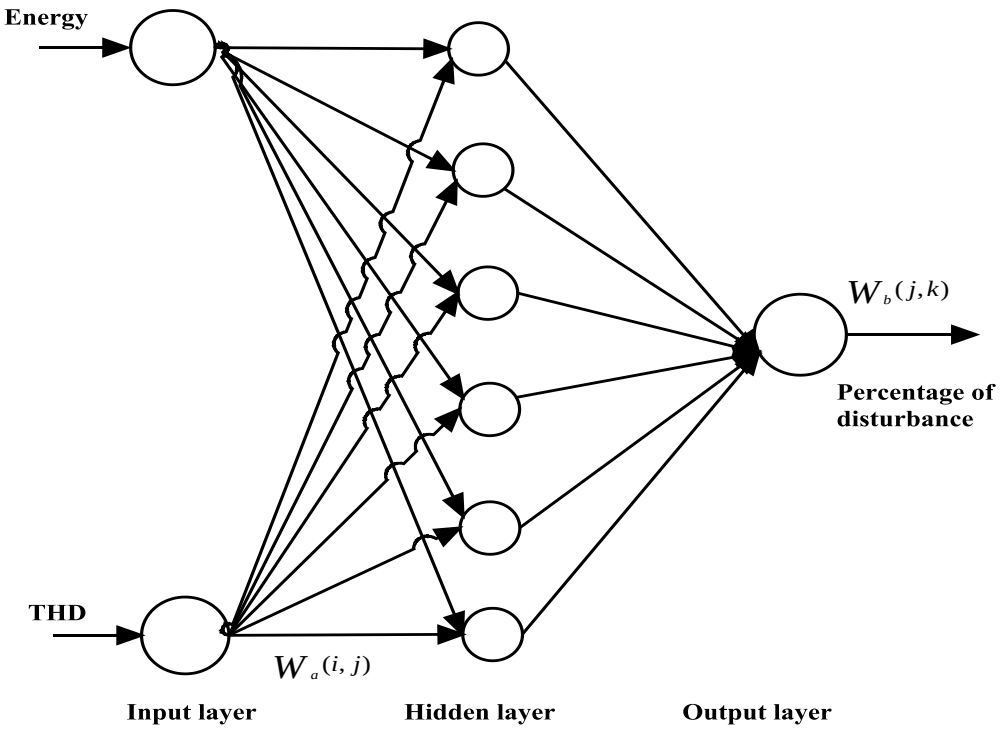


**Figure 5.4 Proposed MFNN Model**

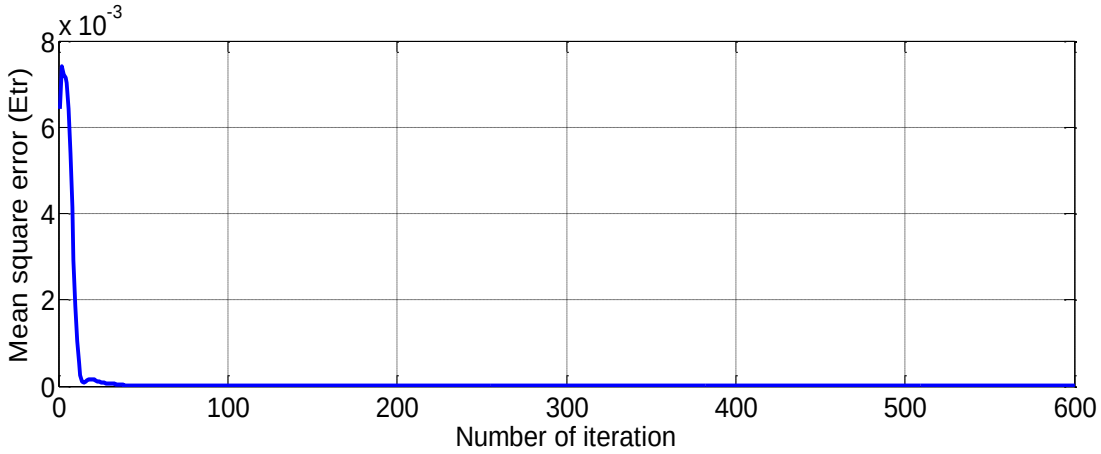


**Figure 5.5 $E_{tr}$ of the training data as a function of Number of iterations**

**Table 5.2: Variation of $E_{tr}$ with η ($N_h$ = 2, α = 0.1, Number of iterations = 600)**

| **η** | **$E_{tr}$** |
|---|---|
| 0.3 | $6.4938*10^{-06}$ |
| 0.4 | $2.9849*10^{-06}$ |
| 0.5 | $1.6490*10^{-06}$ |
| 0.6 | $1.0195*10^{-06}$ |
| 0.7 | $6.7998*10^{-07}$ |
| 0.8 | $4.7907*10^{-07}$ |
| 0.9 | $3.5178*10^{-07}$ |
| **0.99** | **$2.7393*10^{-07}$** |

**Table 5.3: Variation of $E_{tr}$ with α ($N_h$ = 2, η = 0.99, Number of iterations = 600)**

| **α** | **$E_{tr}$** |
|---|---|
| 0.1 | $2.7393*10^{-07}$ |
| 0.2 | $2.1015*10^{-07}$ |
| 0.3 | $1.5616*10^{-07}$ |
| 0.4 | $1.1144*10^{-07}$ |
| 0.5 | $7.5436*10^{-08}$ |
| 0.6 | $4.7389*10^{-08}$ |
| 0.7 | $2.6161*10^{-08}$ |
| 0.8 | $1.0979*10^{-08}$ |
| 0.82 | $8.5030*10^{-09}$ |
| 0.84 | $6.1788*10^{-09}$ |
| **0.85** | **$5.1313*10^{-09}$** |
| 0.86 | $1.3430*10^{-08}$ |
| 0.87 | $1.0390*10^{-06}$ |

**Table 5.4: Variation of $E_{tr}$ with $N_h$ ($\eta = 0.99$, $\alpha_1 = 0.85$, Number of iterations = 600)**

| $N_h$ | $E_{tr}$ |
|---|---|
| 2 | $5.1313*10^{-09}$ |
| 3 | $2.5686*10^{-09}$ |
| 4 | $1.3498*10^{-09}$ |
| 5 | $1.3320*10^{-09}$ |
| **6** | $\mathbf{1.3202*10^{-09}}$ |

Finally, the percentage of disturbance PD = f (e, d) for the test data are calculated by simply passing the input data in the forward path of the network and using the updated weights of the network. Table 5.5 shows a comparison of the exact and the estimated value of percentage of disturbance using this model after 600 iterations**.**

**Table 5.5: Comparison of the exact and estimated value of percentage of disturbance in voltage**

| Type of disturbance | Energy (e) | THD (d) | Percentage of disturbance (%) | Percentage of disturbance(Modeled) | MAE of the test data (%) |
|---|---|---|---|---|---|
| Sag | 1381.8 | 0.7418 | 20 | 20 | 1.7115 |
| | 1251 | 0.7429 | 34 | 34 | |
| | 1158.8 | 0.7438 | 46 | 46 | |
| Swell | 1863.3 | 0.7395 | 118 | 118 | |
| | 2191 | 0.7386 | 138 | 138 | |
| | 2412.2 | 0.7382 | 150 | 149.6276 | |
| Interruption | 972.5855 | 0.7466 | 1.8 | 2.1369 | |
| | 972.9708 | 0.7465 | 2.5 | 2.6298 | |
| | 974.2188 | 0.7460 | 4 | 3.9850 | |
| Sag with harmonics | 3116.1 | 1.5247 | 15 | 15 | |
| | 2949.6 | 1.5779 | 32 | 32 | |
| | 2840.3 | 1.6193 | 46 | 46 | |
| Swell with harmonics | 3575.3 | 1.4156 | 120 | 120 | |
| | 3768.8 | 1.3801 | 132 | 132 | |
| | 4055.5 | 1.3353 | 148 | 149.6885 | |

## 5.5 Summary

In this chapter a PQD detection system is modeled based on the Multilayer Feedforward Neural Network for five different power quality disturbances like sag, swell, interruption, sag with harmonics and swell with harmonics. The features extracted in chapter4 was used as the input-output data for training purposes and percentage of voltage disturbance is estimated and based on this percentage of disturbance the type of disturbance can be easily found out. The results obtained are quite satisfactory which is evident from the low value of mean absolute error obtained in testing of the PQD detection system but it is little slower and takes more time for training if the no of data are more as it is an iterative procedure. The complexity of the system increases as the no of input increases.

## 6.1 Introduction

The Fuzzy logic (FL) refers to a logic system which represents knowledge and reasons in an imprecise or fuzzy manner for reasoning under uncertainity[7].Unlike the classical logic systems, it aims at modeling the imprecise modes of reasoning that play an essential role in human ability to infer an approximate answer to a question based on a store of knowledge that is inexact, incomplete or not totally reliable.it is usually appropriate to use fuzzy logic when a mathematical model does not exist or does exist but is too difficult to encode and too complex to be evaluated fast enough for real time operation. The accuracy of fuzzy logic systems is based on the knowledge of human experts hence, it is only as good as the validity of rules. In this chapter a fuzzy expert system based on certain rules is implemented for classifying different PQ disturbances, before that a brief description of a generalized fuzzy logic system is mentioned in Section 6.2.

## 6.2 Fuzzy logic system

A FL system describes the control action of a process in terms of simple If-Then rules. It describes the algorithm for process control as a fuzzy relation between information on the process conditions to be controlled and the control action. Hence it gives a linguistic or fuzzy model that is developed based on human experience and expertise rather than a mathematical model.in a FL system, the control action is determined from the evaluation of a set of simple linguistic rules. The development of rules requires a thorough understanding of the process to be controlled, but it does not require mathematical model of the system. The model can be single input single output or multi-input multi-output type. The internal structure of a FL system is shown in Figure 6.1.

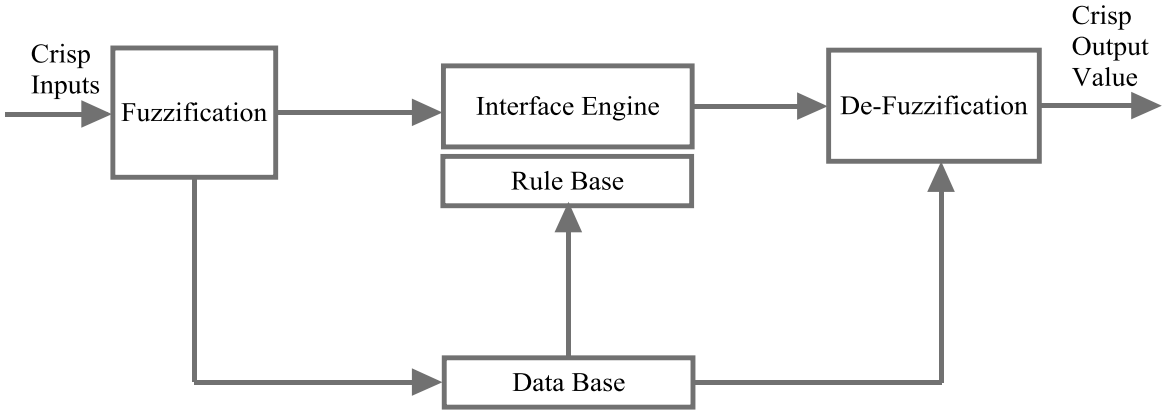


**Figure 6.1 Internal structure of Fuzzy logic system**

The main components of the FL system are:

1. Fuzzification: The FL uses the linguistic variables instead of numerical variables. In the real world, measured quantities are real numbers (crisp).The process of converting a numerical variable into a linguistic variable is called fuzzification.It is classification of input data into suitable linguistic values or sets.
2. Rule Base or Decision Making: This is inferring fuzzy control action from the knowledge of the control rules and the linguistic variable definition. It has 3 different subcomponents.
    - IF (predecessor or antecedent) part of the rule – use of fuzzy operators in it.
    - THEN part of the rule – implication from antecedent part to the subsequent part.
    - Aggregation (accumulation) of the subsequent of all rules. The output of each rule is aggregated to obtain the final output. Some commonly used aggregation methods are Mamdani type implication (Min-Max implication), Lusing Larson type implication and Sugeno type implication. The Mamdani type implication is used for the purpose of classification.
3. Defuzzification: This is the conversion of the inferred fuzzy control action to a crisp or non-fuzzy control action. The choice of defuzzification strategy is a compromise between accuracy and computational intensity. Some of the commonly used methods are Centre of Area method, Height method, Centre of gravity of largest area method and Mean of Maxima method. In this work Centre of Area defuzzification method is used.

## 6.3 Implementation of fuzzy expert system for classification purpose

In this fuzzy expert system the extracted features THD and Energy of different PQ disturbances are used as the input to the fuzzy expert system for classification purpose as shown in Figure 6.2.This Figure is based on the Figure 1.1. The output of the fuzzy expert system will not only classify the type of disturbance, but also it indicates whether the disturbance is pure or contains harmonics.

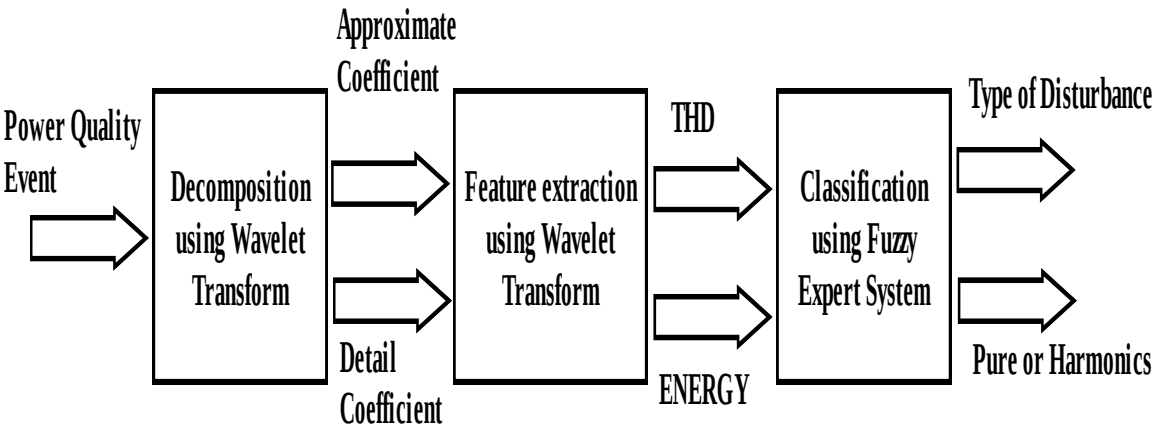


**Figure 6.2 Implementation of fuzzy expert system**

A no of power quality disturbances of various magnitudes have been simulated and corresponding waveforms are obtained. Then two very distinctive features like THD and ENERGY which is inherent to each disturbance is calculated using equation (4.2) and equation (4.4) as discussed in feature extraction. A database of THD and ENERGY of each disturbance at various degree/intensity is prepared. Now based on this database a fuzzy logic system is implemented to classify different power quality disturbances.

### 6.3.1 Membership functions

The Membership functions can have different shapes such as triangular, trapezoidal, Gaussian, bell-shaped, etc. It can be symmetrical or assymetrical.MATLAB facilitates the use of different membership functions with the help of certain syntax. Triangular membership function is the simplest and most commonly used membership function. It can be described by three points forming a triangle. In this work the triangular membership function is used. The fuzzy classification system implemented here has two input variables and two output variables. Input variables are Energy and THD whereas the implications are “Type of disturbance” and “Pure or harmonics” which are the two output variables. Input variable Energy has seven membership functions corresponding to the energy level of different disturbances. Whereas the input variable THD has five membership functions. Output variable1 which indicates type of disturbance has four membership functions and output2 indicates whether the disturbance is pure or contains harmonics has two input variables.

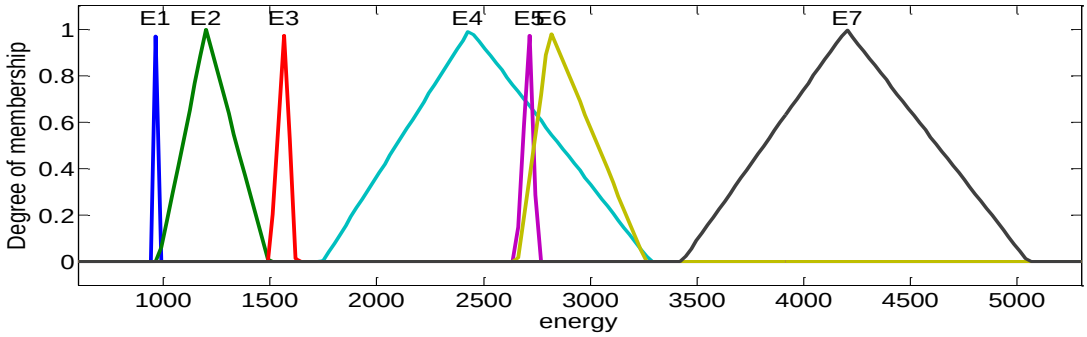


**Figure 6.3 Input membership function of Energy**

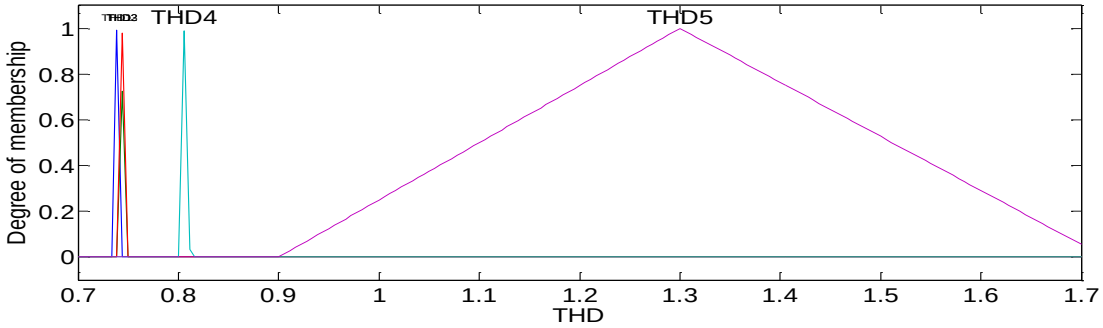


**Figure 6.4 Input membership function for THD**

Figure 6.3 and Figure 6.4 represents the input membership function for Energy and THD respectively. The input1 (Energy) has seven membership functions which in terms of linguistic variables represented as E1, E2, E3, E4, E5, E6 and E7. The input2 (THD) has five membership functions named as thd1, thd2, thd3, thd4 and thd5.

**Table 6.1Relationship between linguistic and actual values for input membership functions**

| Type of disturbance | Energy | Membership function | THD | Membership function |
|---|---|---|---|---|
| Interruption(1% to 9% of fault) | 972.2988 to 982.5388 | E1 | 0.7424 to 0.7467 | thd3 |
| Sag(10% to 90% of fault) | 978.5708 to 1490.6 | E2 | 0.7411 to 0.7464 | thd2 |
| Surge(160% to 240% of fault) | 1615.5 to 1618.7 | E3 | 0.8011 to 0.8113 | thd4 |
| Swell(110% to 190% of fault) | 1746.6 to 3282.6 | E4 | 0.7373 to 0.7399 | thd1 |

| | | | | |
|---|---|---|---|---|
| Interruption with harmonics | 2653.8 to 2752 | E5 | 0.9 to 1.73 | thd5 |
| Sag with harmonics | 2660.1 to 3260 | E6 | 0.9 to 1.73 | thd5 |
| Swell with harmonics | 3428.1 to 5052 | E7 | 0.9 to 1.73 | thd5 |

Table 6.1 shows the relationship between the input variables and membership functions in terms of linguistic variables. Figure 6.5 shows the type of disturbance which has four membership functions representing the type of disturbance such as interruption, sag, swell and surge. Figure 6.6 shows the membership functions for second output which has two membership functions that shows whether the disturbance is pure or contains harmonics.

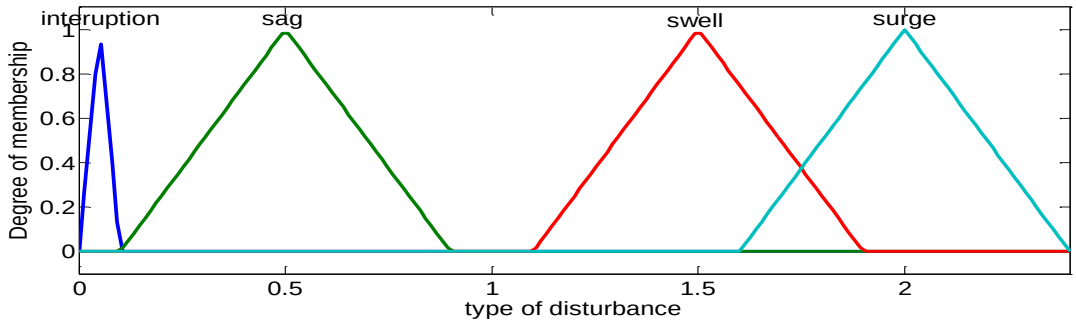


**Figure 6.5 Output membership function 1**

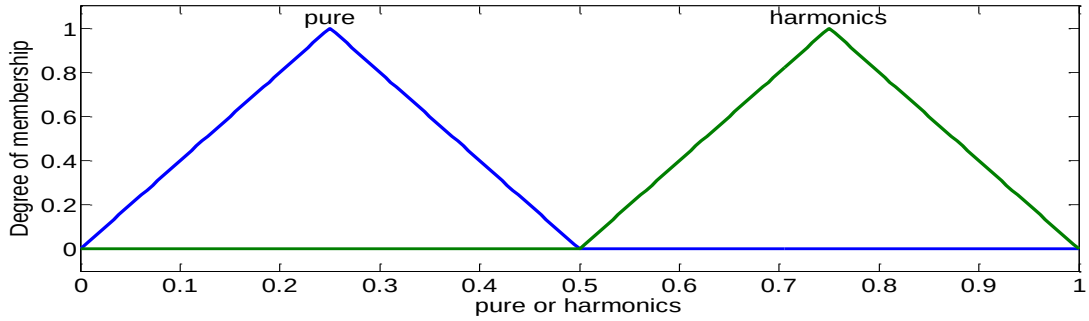


**Figure 6.6 Output membership function 2**

**Table 6.2 Relationship between the linguistic and actual values of output membership function 1 for Type of disturbance.**

| Membership functions for output variable 1 | Percentage of disturbance |
|---|---|
| Interruption | 0.0- 0.09 |
| Sag | 0.1- 0.9 |
| Swell | 1.1- 1.9 |
| Momentary surge | 1.6- 2.4 |

**Table 6.3 Relationship between the linguistic and actual values for output membership function 2**

| Membership function for output variable 2 | Values |
|---|---|
| Pure | 0.0- 0.5 |
| Harmonics | 0.5- 1.0 |

### 6.3.2 Rule base

From the above database following rules are formed for classification purpose.

*Rule1:* If Energy is E1 and THD is thd3, then disturbance is Interruption.

*Rule2:* If Energy is E2 and THD is thd2, then disturbance is Sag.

*Rule3:* If Energy is E3 and THD is thd4, then disturbance is Surge.

*Rule4:* If Energy is E4 and THD is thd1, then disturbance is Swell.

*Rule5:* If Energy is E5 and THD is thd5, then disturbance is Interruption with harmonics.

*Rule6:* If Energy is E6 and THD is thd5, then disturbance is Sag with harmonics.

*Rule7:* If Energy is E7 and THD is thd5, then disturbance is Swell with harmonics.

## 6.4 Classification Accuracy

As many as hundred samples of disturbances in each class of power quality with various magnitudes has been simulated and tested with the above mentioned fuzzy classification system. The overall accuracy obtained is 97%.It shows very little in-accuracy in boundary values of different disturbance band otherwise it gives very accurate results in classifying different disturbances. This system also indicates whether the disturbance contains harmonics or not.Table.6.4 shows the statistical data for the number of samples tested. Equation (6.1) is used for calculating classification accuracy.

$$Classification\ Accuracy(\%) = \frac{X}{Y} \times 100 \tag{6.1}$$

Where X= Number of samples correctly detected Y= Total number of samples considered

**Table.6.4 Classification Accuracy**

| Type of disturbance | No of samples considered(Y) | No of Samples correctly detected(X) |
|---|---|---|
| Interruption | 100 | 98 |
| Sag | 100 | 97 |
| Swell | 100 | 93 |
| Surge | 100 | 98 |
| Sag with harmonics | 100 | 98 |
| Swell with harmonics | 100 | 98 |

## 6.5 Summary

In this chapter a hybrid technique based on the discrete wavelet transform and the Fuzzy Expert system has been proposed for accurate characterization of the power quality disturbances. The main advantage of this proposed technique is to classify the complicated power quality disturbances such as Sag with Harmonics and Swell with Harmonics. The features extracted in Chapter 4 are used as inputs for implementation of the fuzzy expert system based on certain rules. Some difficulties are encountered in classifying the extreme values in each disturbance range correctly. The classification accuracy is the lowest in case of swell disturbance which is about 93% whereas in all other cases it is around 98%. The overall accuracy obtained in classification is found to be 97% which confirms the effectiveness of the system in characterizing different PQ disturbances.

## 7.1 Conclusions

The Detection and classification of PQ disturbances is an important issue in the power quality analysis as before any mitigation action, the type of disturbance and the point of disturbance are needed to take the corrective measure. In this work six different PQ disturbances are considered that includes complex disturbances like sag with harmonics and swell with harmonics for the characterization purpose. First of all these disturbances are decomposed into various levels using wavelet decomposition algorithm of wavelet transform and detected the point of disturbance along with the type of disturbance. This shows that the wavelet transform as a signal processing tool is quite efficient in analysing the PQ disturbances that may be stationary or non-stationary in nature. The WT is a frequency domain approach where the signals are analysed at different frequency resolution levels. The Problem is encountered in detection when the signal is contaminated with a high density of noise or low signal to noise ratio. Also the feature vector to be extracted for the classification purpose will contain high percentage of noise which may degrade the classification accuracy. Hence need arises to de-noise the PQ disturbances before further processing. A wavelet based de-noising technique implementing automatic thresholding rule and soft thresholding function has been proposed. The PQ disturbances are de-noised and the various performance parameters like SNR and MSE were found out to check the efficiency of the method adapted. Then the feature vector is extracted. The two distinct features like THD and Energy are considered for extracting the features. A data base based on the above two features for different PQ disturbances with various magnitude of intensity is prepared. A PQD detection system based on the MFNN is modeled. The features extracted are used as the training patterns and percentage of disturbance is found out and based on this percentage of disturbance the class of disturbance can be easily found out. The mean square error and the mean absolute error are obtained in the training and the testing process respectively. These are found to be satisfactory. Then a fuzzy expert system based on Mamdani Fuzzy interface is designed for the classification of different PQ disturbances. As many as hundred number of PQ events with varying magnitude of fault intensity is generated in each of the PQ disturbance. They are tested with the designed fuzzy expert system to obtain the classification accuracy. The overall classification accuracy obtained with Mamdani Fuzzy Logic is 97% whereas in case of MFNN, mean absolute error obtained is 1.7115% which shows the artificial neural network based system is more efficient. But MFNN is little slower and takes more time for training if the no of data are more as it is an iterative procedure. The Fuzzy

interface system on the other hand faces difficulty in classifying the extreme values in each disturbance range correctly.

## 7.2 Future scope of work

1. In this work only two features like THD and Energy are considered for modeling the PQD detection system using MFNN and fuzzy expert system is used for classification. More features associated with PQ signals like Entropy, standard deviation etc. can be included for modeling as well as classification purpose.

2. Moreover the shape of the membership functions used in fuzzy classification system is triangular in nature more shapes in membership function can be included and the corresponding analysis can be carried out.

3. One more aspect is that in this work the PQ signals are needed to be de-noised first for further processing like detection and feature extraction as wavelet transform as a signal processing tool is quite sensitive to the noise although wavelet based de-noising technique works very well in de-noising but the time elapsed in de-noising cannot be ignored hence research must be carried out to find some other suitable signal processing tool which can overcome this de-noising problem.

## References

[1] Quinquis, “Digital Signal Processing using Matlab,” ISTE WILEY, pp.279-305, 2008.

[2] P.S.Wright,”Short time fourier transform and wigner-ville distributions applied to the calibration of power frequency harmonic analyzers,” *IEEE Trans.instrum.meas.* (1999) 475-478.

[3] Y.Gu,M.Bollen, “Time Frequency and Time Scale Domain Analysis of Voltage Disturbances,” *IEEE Transactions on Power Delivery*, Vol 15, No 4, October 2000, pp 1279-1284.

[4] G.T.Heydt, P.S. Fjeld, C.C.Liu, D.Pierce, L.Tu, G.Hensley,”Applications of the Windowed FFT to Electric Power Quality Assessment,” *IEEE Trans.Power Deliv*.Vol.14 (4) (1999) 1411-1416.

[5] R. Polikar, The Engineer’s Ultimate Guide to Wavelet analysis, The Wavelet Tutorial.March 1999.

[6] S.Santoso, W.M.Grady,E.J.Powers,J.Lamoree and S.C.Bhatt,”characterization of distribution power quality events with fourier and wavelet transforms,” *IEEE Trans.power delivery,*Vol.15,pp 247-254,jan.2000.

[7] Abdelazeem A.Abdelsalam, Azza A.Eldesouky,Abdelhay A.Sallam,”characterization of power quality disturbances using hybrid technique of linear kalman filter and fuzzy expert system,” ELSEVIER Electric power system Reaserch 83 (2012) 41-50.

[8] L.C.Saikia, S.M.Borah, S.Pait,”detection and classification of power quality disturbances using wavelet transform and neural network,” *IEEE annual india conference* 2010.

[9] S. Santoso, E. Powers, W. Grady, and P. Hoffmann,” Power Quality Assessment via Wavelet Transform Analysis,” *IEEE Transactions on Power Delivery*, Vol.11, No.2, pp. 924-930, April 1996.

[10] Peisheng Gao and Weilin Wu, “Power Quality DisturbancesClassification Using Wavelet & Support Vector Machine,” *IEEE Proceedings of the Sixth International Conference on IntelligentSystems Design and Applications* (ISDA'06).

[11] S. Tuntisak and S. Premrudeepreechacharn, “Harmonic Detection in Distribution System Using Wavelet Transform & Support Vector Machine,” *IEEE Conference on Power Tech* 2007.

[12] J.S. Huang, M. Negnevitsky and D.T. Nguyen, "Wavelet transform based harmonic analysis," Australasian universities power engineering Conference and IE Aust Electric Energy Conference, pp.152-156, 1999.

[13] T.K. Abdel-Galil, E. F. EL-Saadany, A.M. Youssef and M. M. A.Salama, "On-line Disturbance Recognition utilizing Vector Quantization based fast match,".

[14] Jaehak Chung, Edward J. Powers, W. Mack Grady and Siddharth C.Bhatt, "Power Disturbance classifier using a Rule-based method and wavelet packet based hidden Markov model, " *IEEE transactions on power delivery,* Vol. 17, no. 1, January 2002.

[15] Boris Bizjak and Peter Planinsic, "Classification of PowerDisturbances using Fuzzy Logic,".

[16] Atish K. Ghosh and David L. Lubkeman, "The Classification of Power System Disturbance waveforms using a Neural Network Approach," *IEEE Transactions on Power Delivery,* Vol. 10, No. 1, January 1995.

[17] Surya Santoso, Edward J. Powers, and W. Mack Grady and Antony C.Parsons, "Power Quality Disturbance Waveform Recognition Using Wavelet-Based Neural Classifier—Part 1: Theoretical Foundation," *IEEE transactions on power delivery,* Vol. 15, no. 1, January 2000.

[18] D.Tianjun, C.Guangju and Y.Lei," Frequency Domain Interpolation Wavelet Transform based Algorithm for Harmonic Analysis of Power System," ICCCAS2004 International Conference on Communications, Circuits and Systems, Vol.2, pp.742-746, 27-29 June 2004.

[19] Sudipta Nath,Priyanjali Mishra,"Wavelet based Feature Extraction for Classification of Power Quality Disturbances," ICREPQ'11 International Conference on Renewable Energies and Power Quality,13-15 April,2011.

[20] Wei Bing Hu, Kai Cheng Li, Dang Jun Zhao, Bing Ruo Xie, "Performance Improvement of Power Quality Disturbance Classification Based on a New Denoising Technique," Proceeding of International Conference on Electrical Machines and Systems 2007, Oct. 8~11, Seoul, Korea.

[21] Chuah keow, P.Nallagownden, K.S. Rama Rao, "De-noising scheme for enhancing power quality problem classification based on wavelet transform and a rule-based method," International Conference on Electrical, Control and Computer Engineering,Malaysia,June201 Pahang, Malaysia, June 21-22, 2011.

[22] Gu Jie, "Wavelet Threshold De-noising of Power Quality Signals," 2009 Fifth International Conference on Natural Computation.